bioRxiv preprint doi: https://doi.org/10.1101/760892; this version posted April 25, 2021. The copyright holder for this preprint (which was not certified by peer review) is the author/funder, who has granted bioRxiv a license to display the preprint in perpetuity. It is made available under aCC-BY-NC-ND 4.0 International license.

Title: The circadian clock gene circuit controls protein and phosphoprotein rhythms in *Arabidopsis thaliana*.

Short title: Clock gene regulation of the Arabidopsis (phospho)proteome

Authors:

Dr Johanna Krahmer[1,2,5], Dr Matthew Hindle[3], Dr Laura K Perby[4], Prof Tom H Nielsen[4], Prof Karen J Halliday[2], Dr Gerben van Ooijen[2], Dr Thierry Le Bihan[1], Prof Andrew J Millar[1]

Affiliations:

[1]SynthSys and School of Biological Sciences, CH Waddington Building, Max Born Crescent, Kings Buildings, University of Edinburgh, Edinburgh, EH9 3BF, United Kingdom

[2]Institute for Molecular Plant Science, School of Biological Sciences, Daniel Rutherford Building, Building, Max Born Crescent, Kings Buildings, University of Edinburgh, Edinburgh, EH9 3BF, United Kingdom

[3]The Roslin Institute and Royal (Dick) School of Veterinary Studies, Easter Bush, Edinburgh, EH25 9RG, United Kingdom

[4]Department of Plant and Environmental Sciences, University of Copenhagen, Section for Molecular Plant Biology, Thorvaldsensvej 40, DK-1871 Frederiksberg C, Denmark

[5]Present address: Center for Integrative Genomics, Faculty of Biology and Medicine, University of Lausanne, 1015 Lausanne, Switzerland

Corresponding author information:

Johanna Krahmer, email: johanna.krahmer@unil.ch

Andrew J Millar, email: Andrew.Millar@ed.ac.uk

ORCID:

Johanna Krahmer: 0000-0001-7728-5110

bioRxiv preprint doi: https://doi.org/10.1101/760892; this version posted April 25, 2021. The copyright holder for this preprint (which was not certified by peer review) is the author/funder, who has granted bioRxiv a license to display the preprint in perpetuity. It is made available under aCC-BY-NC-ND 4.0 International license.

Matthew Hindle: 0000-0002-6870-4069

Andrew Millar: 0000-0003-1756-3654

Gerben van Ooijen: 0000-0001-7967-0637

Abbreviations:

TTFL	Transcriptional translational feedback loop
NTO	non-transcriptional oscillator
F2KP	fructose-6-phosphate-2-kinase / phosphatase
CCA1	Circadian clock associated 1
CCA1-OX	CCA1 overexpressor
CK	casein kinase
SNF-1	sucrose non-fermenting
SnRK	SNF-1 related kinase
TOC1	timing of CAB expression 1
TOC1-Ox	TOC1 overexpressor
PRX	peroxiredoxin
PCA	principal component analysis
Col-0	Columbia 0
ZT	Zeitgeber time
h	hour
WT	wildtype
GO	gene ontology
SEM	standard error of the mean
BH	Benjamini - Hochberg

Abstract

24-hour, circadian rhythms control many eukaryotic mRNA levels, whereas the levels of their more stable proteins are not expected to reflect the RNA rhythms, emphasizing the need to test the circadian regulation of protein abundance and modification. Here we present circadian

bioRxiv preprint doi: https://doi.org/10.1101/760892; this version posted April 25, 2021. The copyright holder for this preprint (which was not certified by peer review) is the author/funder, who has granted bioRxiv a license to display the preprint in perpetuity. It is made available under aCC-BY-NC-ND 4.0 International license.

proteomic and phosphoproteomic time-series from *Arabidopsis thaliana* plants under constant light conditions, estimating that just 0.4% of quantified proteins but a much larger proportion of quantified phospho-sites were rhythmic. Approximately half of the rhythmic phospho-sites were most phosphorylated at subjective dawn, a pattern we term the 'phospho-dawn'. Members of the SnRK/CDPK family of protein kinases are candidate regulators. A *CCA1*-over-expressing line that disables the clock gene circuit lacked most circadian protein phosphorylation. However, the few phospho-sites that fluctuated despite *CCA1*-over-expression still tended to peak in abundance close to subjective dawn, suggesting that the canonical clock mechanism is necessary for most but perhaps not all protein phosphorylation rhythms. To test the potential functional relevance of our datasets, we conducted phosphomimetic experiments using the bifunctional enzyme fructose-6-phosphate-2-kinase / phosphatase (F2KP), as an example. The rhythmic phosphorylation of diverse protein targets is controlled by the clock gene circuit, implicating post-translational mechanisms in the transmission of circadian timing information in plants.

Keywords

circadian clock; non-transcriptional oscillator; Arabidopsis; phosphoproteomics

Introduction

Most circadian observations in the well-characterised plant species *Arabidopsis thaliana* can be explained by a genetic network of mostly negatively interacting transcription factors (1,2). In addition to transcriptional interactions, this transcriptional-translational feedback loop (TTFL) system requires post-translational modification of transcription factor proteins (3). Phosphorylation of CCA1 by casein kinase (CK) 2 for example is necessary for the circadian clock function (4).

Protein phosphorylation is involved in the circadian clock mechanism not only in plants but also in fungi, animals and cyanobacteria (3,5). While the transcription factors of TTFLs in animals, fungi and plants are not evolutionarily conserved (3), many kinases that play a role

bioRxiv preprint doi: https://doi.org/10.1101/760892; this version posted April 25, 2021. The copyright holder for this preprint (which was not certified by peer review) is the author/funder, who has granted bioRxiv a license to display the preprint in perpetuity. It is made available under aCC-BY-NC-ND 4.0 International license.

in circadian timekeeping are similar across eukaryotes. For instance CK2 is also important for circadian timing in mammals (6) and fungi (7). Protein phosphorylation is also involved in the output of the circadian clock (8). However, only one study has so far addressed the question of how pervasive circadian protein phosphorylation is in higher plants (9).

In circadian biology, transcriptional studies have long dominated research efforts, leading to the well-established TTFL models (e.g. refs (1,2,10–12)). However, it has become apparent that protein abundance and post-translational modification cannot be ignored, since these do not simply follow transcript expression patterns (e.g. refs. (13–15)). There is even evidence that circadian oscillations can be driven by non-transcriptional oscillators (NTOs) that are independent of rhythmic transcription. The cyanobacterial circadian clock is based on rhythmic autophosphorylation of the KaiC protein together with the KaiA and KaiB proteins and this mechanism does not even require a living cell to create oscillations (16). Evidence for NTOs also exists in eukaryotes; the protein peroxiredoxin (PRX) is rhythmically over-oxidized in the absence of transcription in algae and human red blood cells (17,18). Circadian rhythms of PRX over-oxidation were also observed in organisms that have impaired circadian oscillators, in mutants of the fungus *Neurospora crassa* and in transgenic Arabidopsis plants (19). The circadian PRX over-oxidation rhythm even exists in cyanobacteria and archaea (19). In addition, circadian magnesium and potassium ion transport has been observed across eukaryotes and can occur in transcriptionally inactive *Ostreococcus tauri* and human red blood cells (20,21). Therefore, at least some eukaroytes possess NTOs that appear to be evolutionarily ancient and conserved (3).

With mass spectrometer technology becoming more and more advanced, several circadian proteomics studies have been conducted in different species, such as proteomics analyses of protein abundance time courses (15,22–25), proteomics specifically at the day / night transition (25,26) or circadian phosphoproteomics (9,24).

In this study, we used mass spectrometry based proteomics and phosphoproteomics on

bioRxiv preprint doi: https://doi.org/10.1101/760892; this version posted April 25, 2021. The copyright holder for this preprint (which was not certified by peer review) is the author/funder, who has granted bioRxiv a license to display the preprint in perpetuity. It is made available under aCC-BY-NC-ND 4.0 International license.

112 circadian time courses to address the following questions: (1) How pervasive are rhythms in
113 protein abundance and phosphorylation as a clock output in a normally functioning circadian
114 clock system, and what are the characteristics of such rhythms? and (2) can protein abundance
115 or phosphorylation be rhythmic in a plant with a disabled transcriptional oscillator? To
116 investigate (1), we used a time course of WT plants, and for addressing (2), we generated time
117 courses from plants overexpressing the *CIRCADIAN CLOCK-ASSOCIATED 1* gene (CCA1-
118 OX), which have an impaired TTFL. We generated global proteomics and phosphoproteomics
119 data in parallel from the same protein extracts. Our analysis revealed that the transcriptional
120 oscillator is required for most rhythmic protein phosphorylation, and that most rhythmic
121 phosphopeptides peak at subjective dawn. We also found this 'phospho-dawn' trend among
122 the time courses of fluctuating phosphopeptides in the CCA1-OX. Finally, we selected a
123 phosphosite of the bifunctional enzyme fructose-6-phosphate-2-kinase / fructose-2,6-
124 bisphosphatase (F2KP) to illustrate how our data can be used to study the mechanisms of
125 clock output pathways that connect to central carbon metabolism.
126
127 **Experimental Procedures**
128
129 *Plant material*
130 *Arabidopsis thaliana* WT (Col-0 accession) and a *CCA1* over-expressing plants ('CCA1-OX',
131 (27)) were used in this study. Seeds were germinated and grown on plates (2.15g/l Murashige
132 & Skoog medium Basal Salt Mixture (Duchefa Biochemie), pH 5.8 (adjusted with KOH) and
133 12g/l agar (Sigma)) at 85µmol m^{-2} s^{-1} white fluorescent lights at 21°C in Percival incubators
134 for 11 days in 12h light, 12h dark cycles. Seedlings were transferred to soil and grown for 11
135 more days at a light intensity of 110µmol m^{-2} s^{-1} in the same light-dark cycle.
136
137 *Experimental Design and Statistical Rationale*
138 After plants had grown for a total of 22 days, from ZT 0 of day 23 lights remained switched
139 on continuously and collection of plant material started at ZT 12 (dataset I) or ZT 24 (dataset

bioRxiv preprint doi: https://doi.org/10.1101/760892; this version posted April 25, 2021. The copyright holder for this preprint (which was not certified by peer review) is the author/funder, who has granted bioRxiv a license to display the preprint in perpetuity. It is made available under aCC-BY-NC-ND 4.0 International license.

II). In dataset I, six time points at 4h intervals were taken with five replicates for each time point, harvesting eight rosettes for the WT and 12 rosettes for the CCA1-OX. In dataset II, also at 4h intervals, at least six replicates of eight rosettes each were taken for the WT, five (16 rosettes each) of the CCA1-OX. In dataset I, the time course was sampled from ZT12 to ZT32, in dataset II from ZT24 to 48 (CCA1-OX) or ZT24 to ZT52 (WT).

Statistical analysis of time courses required assessment of not only changes but also rhythmicity. We therefore used both analysis of variance (ANOVA) and JTK_CYCLE as statistical tools (see below for details).

Sample preparation

Rosettes without roots were harvested by flash-freezing in liquid nitrogen. Protein extraction and precipitation was carried out according to method 'IGEPAL-TCA' described by (28). Briefly, protein was extracted and precipitated with TCA and phase separation, then washed with methanol and acetone. 500µg re-suspended protein was digested using a standard in-solution protocol and peptides were desalted. Before drying, eluted peptides were separated into two parts: 490µg of the digest was used for phosphopeptide enrichment, 10µg was saved for global protein analysis. Phosphopeptides were enriched using the Titansphere™ spin tip kit (GL Sciences Inc.) and desalted on BondElut Omix tips (Agilent) according to the manufacturers' instructions.

Mass spectrometry, peptide merging and Progenesis analysis

LC-MS/MS measurement and subsequent analysis by the Progenesis software (version 4.1.4924.40586) was carried out as previously described (28): Dried peptides were dissolved in 12 µl (phosphoproteomics) or 20µl (global proteomics) 0.05% TFA and passed through Millex-LH 0.45µm (Millipore) filters. 8 µl were run on an on-line capillary- HPLC-MSMS system consisting of a micropump (1200 binary HPLC system, Agilent, UK) coupled to a hybrid LTQ-Orbitrap XL instrument (Thermo-Fisher, UK). Reverse phase buffer used for LC-MS separation was buffer A (2.5% acetonitrile, 0.1% FA in H_2O) and buffer B (10%

bioRxiv preprint doi: https://doi.org/10.1101/760892; this version posted April 25, 2021. The copyright holder for this preprint (which was not certified by peer review) is the author/funder, who has granted bioRxiv a license to display the preprint in perpetuity. It is made available under aCC-BY-NC-ND 4.0 International license.

168 H_2O, 90% acetonitrile, 0.1% formic acid, 0.025% TFA). LC peptide separation was carried
169 out on an initial 80 min long linear gradient from 0% to 35% buffer B, then a steeper gradient
170 up to 98% buffer B over a period of 20 min then remaining constant at 98% buffer B for 15
171 min until a quick drop to 0% buffer B before the end of the run at 120 min.
172 The tair Arabidopsis_1rep (version 20110103, 27416 protein entries) database was used for
173 data-dependent detection, using the Mascot search engine (version 2.4), including all peptide
174 sequences of rank smaller than 5. Search parameters were as follows: charges 2+, 3+ and 4+,
175 trypsin as enzyme, allowing up to two missed cleavages, carbamidomethyl (C) as a fixed
176 modification, Oxidation (M), Phospho (ST) and Phospho (Y), Acetyl(Protein N-term) as
177 variable modifications, a peptide tolerance of 7 ppm, and MS/MS tolerance of 0.4 Da, peptide
178 charges 2+, 3+, and 4+, on an ESI-trap instrument, with decoy search and an ion-cutoff of 20.
179 In all but one cases, these parameters resulted in a false-discovery rate (FDR), of less than 5%
180 with one exception (phosphoproteomics dataset I: 3.5%, phosphoproteomics dataset II: 3.2,
181 global dataset I: 6.8%, global dataset II: 4.5%, calculated using the formula 2*d/(n+d) (29), n
182 and d being the number of hits in the normal and decoy databases, respectively, using an ion
183 score cutoff of 20). Peptides were quantified by their peak area by Progenesis, and proteins
184 were quantified by using the sum of the quantitation of all unique peptides. Where peptides
185 matched very similar proteins, multiple accession numbers are shown in exported results from
186 Progenesis (Supplementary Data S1, S2).
187 In order to remove duplicates of phosphopeptides due to alternative modifications other than
188 phosphorylation or missed cleavages, we used the qpMerge software following the Progenesis
189 analysis (30). The data are publicly available in the pep2pro database (31) at http://fgcz-
190 pep2pro.uzh.ch (Assembly names ‘ed.ac.uk Global I’, ‘ed.ac.uk Global II’, ‘ed.ac.uk Phospho
191 I’, ‘ed.ac.uk Phospho II’) and have been deposited to the ProteomeXchange Consortium
192 (http://proteomecentral.proteomexchange.org) via the PRIDE partner repository (32) with the
193 dataset identifier PXD009230. Exported .csv files from Progenesis with all peptide and
194 protein quantifications can be found in the online supplementary material (Data S1 and S2).
195

bioRxiv preprint doi: https://doi.org/10.1101/760892; this version posted April 25, 2021. The copyright holder for this preprint (which was not certified by peer review) is the author/funder, who has granted bioRxiv a license to display the preprint in perpetuity. It is made available under aCC-BY-NC-ND 4.0 International license.

General statistics and outlier removal

Results of statistical analyses are summarised in Data S3. Outlier analysis, statistics and Venn diagrams were done using R version 3.2.1 (33). Zero values for the quantification were exchanged for 'NA'. For outlier analysis and parametric tests such as ANOVA, arcsinh transformed data was used to obtain a normal distribution, while untransformed data was used for plotting time courses and for the non-parametric JTK_CYCLE analysis. For phosphoproteomics analysis all replicates in which the Pearson correlation coefficient among replicates of the same time point was lower than 0.8 were regarded as outliers (supplementary methods, Supplementary Data S4). In global dataset II, the first run replicate of each time point had to be excluded as an outlier due to an apparent drift (Supplementary Data S4). To generate heat maps, the abundance of each peptide or protein was normalized by the time course mean of the peptide or protein, followed by taking the log2 to centre values around 0, and the heatmap.2 function from the pvclust R package was applied (34).

JTK_CYCLE analysis

We used the R-based tool JTK_CYCLE (35) to determine rhythmicity, with the following modifications: (1) we ran the JTK_CYCLE algorithm for each phosphosite or protein separately rather than the entire list, to allow handling of missing quantification values for some replicates. Benjamini Hochberg (BH) (36) correction of p-values was carried out after application of the JTK_CYCLE tool. (2) Since our time course durations are close to the periods of rhythms we are searching for, some identifications were assessed as rhythmic by the original JTK_CYCLE tool that were increasing or decreasing continually over the entire time course. We excluded these from the group of rhythmic identifications ('excl.' in p-value column in Supplementary Data S5). For dataset-wide analyses we used $p<0.05$ as a cutoff for rhythmicity and then trusted results that agree between experiments. Similarly, for judging individual time courses we focus on those with $p < 0.05$ in both datasets.

Kinase prediction using GPS3.0

bioRxiv preprint doi: https://doi.org/10.1101/760892; this version posted April 25, 2021. The copyright holder for this preprint (which was not certified by peer review) is the author/funder, who has granted bioRxiv a license to display the preprint in perpetuity. It is made available under aCC-BY-NC-ND 4.0 International license.

Kinases for each site were predicted using the *Arabidopsis thaliana* specific GPS 3.0 prediction tool in its species specific mode for *Arabidopsis thaliana* (37,38). For each phosphorylation site, an amino acid sequence was generated that contained 50 amino acids on either side of the phosphorylated residue using a python script. This resulted in 101 amino acid long sequences, unless the phosphosite was closer than 50 residues to the C or T terminus in which case the missing positions were filled by 'X'. The phosphopeptides used as foreground were the significantly rhythmic phosphosites (JTK_CYCLE p-value < 0.05) peaking at a given time point, all other phosphosites identified in the same experiment were used as background. The high threshold setting was used to minimize false-positive predictions and searches were done for S and T residues. In order to reduce the complexity of the dataset, we used a simplification: where kinases from different families were predicted, only the one with the highest difference between score and cutoff was used. For foreground and background the numbers of predictions for each occurring kinase group were counted and the Fisher's Exact test was used to determine predicted kinases that were significantly enriched in the foreground group ($p<0.05$).

GO analysis

For GO analysis, foreground and background were chosen as in the kinase prediction analysis. With these groups, GO analysis was conducted using the topGO script (39), followed by Fisher's exact test to determine enrichment of terms (supplementary data S6).

Generation of F2KP point mutations and expression constructs

The F2KP coding sequence in the pDONR221 vector, lacking a stop codon, was kindly provided by Dr Sebastian Streb, ETH Zürich. The QuikChange Lightning Site-Directed Mutagenesis kit (Agilent Technologies) was used to introduce point mutations using primer pair AspF and AspR for mutation of S276 to aspartic acid or AlaF and AlaR for mutation to alanine (Table S 4). The WT or mutated F2KP coding sequences were amplified by PCR using primers F2KP-F and F2KP-R (Table S 4), introducing restriction sites for AflII (3' end)

bioRxiv preprint doi: https://doi.org/10.1101/760892; this version posted April 25, 2021. The copyright holder for this preprint (which was not certified by peer review) is the author/funder, who has granted bioRxiv a license to display the preprint in perpetuity. It is made available under aCC-BY-NC-ND 4.0 International license.

and XbaI (5' end) and a stop codon. Using these restriction sites, digested PCR products were ligated into the pmcnEAVNG expression vector which allows expression in *E.coli* with an N-terminal GST tag and a T7 promoter for IPTG inducibility. Plasmids were transformed into Rosetta™2(DE3)pLysS Competent expression strain (Novagen).

Expression of GST-F2KP constructs in E. coli cells

The three constructs, WT, S276E and S276A were expressed in *E.coli* and purified using the GST tag. Two independent expression experiments were performed (experiment 1 and experiment 2), each in triplicates. 200ml *E.coli* cultures were grown at 37°C with 100µg/ml ampicillin and 25µg/ml chloramphenicol and induced with 1mM IPTG at OD_{600} values between 0.6 and 0.8. Cells were harvested by centrifugation after 2.5h of expression at 37°C. Each pellet was from 50ml bacterial culture. For purification of GST-F2KP, pellets were lysed in 2.5ml PBS with Complete protease inhibitor cocktail (Roche) with a probe sonicator. After clearing of the lysates, AP was carried out using GSH-agarose beads, with 167µl GSH-agarose bead suspension (Protino glutathione agarose 4B, Macherey-Nagel), a binding incubation of 30min at room temperature, 4 washes with 10x the volume of the bead suspension and elution in PBS with 100mM reduced glutatione (pH 8.0) 3 times 30min at room temperature.

F2KP activity assay

F2KP activity of purified F2KP was measured as described in (40) (F-2,6-BP producing reaction) and (41) (measurement of generated F-2,6-BP by its activation of PFP and subsequent production of NADH produced from glycolytic enzymes).

Western blot quantification of F2KP concentration in AP eluates

To test whether the differences in F2KP activity of eluates could be caused by differences in abundance in the eluate, we quantified the amount of F2KP in equal volumes of eluates by western blotting. Samples were prepared for SDS-PAGE with 25% 4xLDS (Life

bioRxiv preprint doi: https://doi.org/10.1101/760892; this version posted April 25, 2021. The copyright holder for this preprint (which was not certified by peer review) is the author/funder, who has granted bioRxiv a license to display the preprint in perpetuity. It is made available under aCC-BY-NC-ND 4.0 International license.

Technologies, NP0008) and 20mM DTT and were incubated at 70°C for 10min. Two concentration series of an equal mix of all three eluates were loaded on each gel for relative quantitation. Individual eluates were examined in duplicates (expression 1) or triplicates (expression 2). 4-12% Bis-Tris Gels (Life Technologies) were run and protein was blotted onto nitrocellulose membrane using the iBlot® system. Two primary antibodies were used in parallel: anti-F2KP from rabbit, raised against amino acids 566-651 (42) and anti-GST from mouse (Thermo Scientific), both at a dilution of 1:1,000 overnight. Secondary antibodies were goat-anti-rabbit (IRDye®800CW, LI-COR) and goat-anti-mouse (IRDye®680RD, LI-COR). Bands were quantified using the ImageStudioLite (version 2) software.

bioRxiv preprint doi: https://doi.org/10.1101/760892; this version posted April 25, 2021. The copyright holder for this preprint (which was not certified by peer review) is the author/funder, who has granted bioRxiv a license to display the preprint in perpetuity. It is made available under aCC-BY-NC-ND 4.0 International license.

Results

Circadian protein phosphorylation requires the canonical transcriptional oscillator

We generated global proteomics and phosphoproteomics datasets for two independent circadian time courses and for two genotypes each – WT and the CCA1-OX line which has an impaired circadian oscillator (27). This resulted in four datasets: global protein and phosphopeptide datasets I (Zeitgeber time (ZT) 12 to ZT32) and datasets II (ZT24 to ZT48 (CCA1-OX) or ZT52 (WT)) (Figure 1A,B). We removed outliers before conducting further statistical analysis (Supplementary Data S4).

We identified 2287 phosphopeptides in dataset I, 1664 in dataset II, which condensed to between 1000 and 1500 in each dataset after applying qpMerge (30) to remove duplicate phosphopeptides (Table 1A). These were from several hundred proteins in each dataset and over 1000 in both datasets together (Table 1B). In the global protein analysis, we identified 1896 and 1340 proteins in dataset I and II, respectively, adding up to a total of 2501 for both datasets combined (Table 1A,B). To assess the circadian rhythmicity of each phosphopeptide or protein, we employed the non-parametric JTK_CYCLE method (35) as it can be applied to time courses of only one cycle, taking the curve shape into account. Unless otherwise stated we considered periods of 22 to 26h and excluded continuously increasing or decreasing profiles from the group of rhythmic phosphopeptides or proteins. In dataset I, 606 (40%) phosphopeptides were rhythmic in the WT, in dataset II 100 (8.8%) based on the p-value of the individual timeseries. 338 (23%) (dataset I) and 26 (2.3%) (dataset II) were rhythmic after adjusting for multiple testing ('q-value' < 0.05) (36). The fraction of rhythmic proteins in the global proteomics analysis was smaller than in the case of phosphopeptides: 171 (9.0%) in dataset I, 45 (3.4%) in dataset II had JTK_CYCLE p-values < 0.05. 6 proteins also had q-value < 0.05 in each dataset (0.32% in dataset I, 0.45% in dataset II). Phosphopeptides and proteins with JTK_CYCLE p<0.05 in both datasets are listed in Table 2.

bioRxiv preprint doi: https://doi.org/10.1101/760892; this version posted April 25, 2021. The copyright holder for this preprint (which was not certified by peer review) is the author/funder, who has granted bioRxiv a license to display the preprint in perpetuity. It is made available under aCC-BY-NC-ND 4.0 International license.

In the CCA1-OX line, 37 (2.5%) phosphopeptides had a JTK_CYCLE p-value < 0.05 in dataset I, 17 (1.5%) in dataset II; in the global datasets, 122(6.4%) and 57 (4.3%) had a JTK_CYCLE p-value < 0.05 in datasets I and II, respectively. After adjusting for multiple testing, only two significant identifications remained for the CCA1-OX phosphopeptides in dataset I and none in dataset II (Table 1A). This analysis suggests that a functional TTFL is required for most rhythmic protein phosphorylation.

For further whole-dataset analyses, we used JTK_CYCLE p-value < 0.05 as a criterion for rhythmicity and treated results as reliable if rhythmic scores were obtained from separate analysis of each dataset. This approach is also supported by comparison with existing data: Among the phosphopeptides with $p < 0.05$ and $q>0.05$ were phosphosites that were previously shown to be rhythmic with almost identical phases, such as RTT(pS)LPVDAIDS of WITH NO LYSINE (WNK) 1, and TL(pS)STPLALVGAK of CHLORIDE-CHANNEL-A (CLC-A) (Supplementary Data S3) (9).As expected, the global proteomic analysis did not quantify all the proteins identified by the phosphoproteomic enrichment (Figure 1 C,E). We found very few proteins with rhythms in abundance as well as rhythmic phosphopeptides (12 in dataset I, 2 in dataset II). About half of the rhythmic phosphopeptides or proteins had rhythmic transcripts (Figure 1D,F).

Since *CCA1* is a morning-expressed gene, the CCA1-OX line might be expected to have a 'morning-locked' circadian oscillator. To test whether this observation applies at the protein abundance and phosphorylation level, we calculated the absolute value of the difference between CCA1-OX and WT (|CCA1-OX - WT|) at each dawn and dusk time point (i.e. ZT12, 24, 36 and 48) for time courses of all proteins or phosphopeptides that were rhythmic in WT (p-value <0.05) and quantified in CCA1-OX. For each dawn – dusk pair, we determined whether the difference between CCA1-OX and WT was larger at dusk or at dawn and counted the number of such pairs as a coarse indication of the difference between the proteome or phosphoproteome of these two genotypes, for each dataset and time point pair (Table S 1).

bioRxiv preprint doi: https://doi.org/10.1101/760892; this version posted April 25, 2021. The copyright holder for this preprint (which was not certified by peer review) is the author/funder, who has granted bioRxiv a license to display the preprint in perpetuity. It is made available under aCC-BY-NC-ND 4.0 International license.

CCA1-OX differed more from the WT at dusk rather than dawn, in all but one of the time point pairs (the exception was one of the smallest pairs, in global dataset II). This is consistent with a partially morning-locked circadian clock at the protein (modification) level, as expected from the role of CCA1 in the TTFL. The consistency of the dataset supports our interpretation, from the very few rhythmic identifications in CCA1-OX, that the TTFL is necessary for most of the rhythms observed in WT plants.

Circadian rhythms of proteins in the global proteomics datasets

We applied GO analysis to the global proteomics data, using rhythmic proteins at each peak time point as foreground and all other identified proteins as background (Supplementary Data S6). In both datasets, enriched GO terms in the WT at the end of the subjective day (ZT12 and ZT36) were photosynthesis related terms, 'response to glucose', 'regulation of protein dephosphorylation' and oxidoreductase activity with NAD or NADP as acceptor. The latter was also enriched in the CCA1-OX in dataset I. In addition, in the CCA1-OX, two terms related to cell wall metabolic processes were enriched in both datasets during the subjective night (ZT20 and ZT44) (Supplementary Data S6).

Among rhythmic proteins shared between the datasets, we identified six for the WT, three for the CCA1-OX (Table 2D,E). One protein, INOSITOL 3-PHOSPHATE SYNTHASE 1 (MIPS1, AT4G39800) was rhythmic with a peak at 24-28h in both datasets and both genotypes but with lower p-value and higher amplitude in the WT (Figure 2A). Two other examples of high-confidence rhythms in protein abundance are chloroplast BETA-AMYLASE 3 (BAM3) (Figure 2B) and the light-harvesting chlorophyll a/b binding protein LHCB2.2 (Figure 2C).

WT phosphoproteomics data reveals rhythmic phosphoproteins with a variety of functions, including previously unknown phosphosite rhythms

bioRxiv preprint doi: https://doi.org/10.1101/760892; this version posted April 25, 2021. The copyright holder for this preprint (which was not certified by peer review) is the author/funder, who has granted bioRxiv a license to display the preprint in perpetuity. It is made available under aCC-BY-NC-ND 4.0 International license.

GO term enrichment within the peak time groups of the phosphoproteomics data revealed that only one GO term ('cotyledon development') was shared between the two datasets and the ZTs of enrichment are 16 h apart (Supplementary Data S6). Several terms were shared between the WT and the CCA1-OX in dataset I, most of them related to energy metabolism or ion homeostasis, and all of them were enriched at ZT24 or ZT28. Apart from overlap of exact GO IDs, we found enrichment of terms related to translation in the WT at 24h in both phosphoproteomics datasets, which is consistent with rhythmic phosphorylation of RPS6 isoforms (Supplementary data S6, Table 2, Data S3) (9).

In agreement with the small number of consistently enriched GO terms and with (9), we found that the proteins for which we found rhythmic phosphosites in the WT are associated with a large variety of functions, such as translation initiation (RPS6A, RPS6B), nitrogen / amino acid metabolism or transport (NIA2, NRT1.7, CLC-A), light harvesting (CAB4) or flowering (COL-9).

In our datasets we also found previously unknown phosphosite rhythms, such as on ASPARAGINE SYNTHETASE (ASN) 2, SWEET12, PLASMA MEMBRANE INTRINSIC PROTEIN (PIP) 2;7 and VARICOSE RELATED (VCR) (Figure 3, and see discussion).

Very few proteins are rhythmically phosphorylated in the CCA1-OX

Only 2 phosphopeptides with $p<0.05$ for the CCA1-OX appear in both datasets (Table 2B): A phosphopeptide of a Leucine rich repeat protein kinase (AT2G33830) and a dormany/auxin associated family protein (AT1G51805). The latter showed a significant increase in its total protein abundance in dataset I (Table 2B), therefore changes may be due to increasing protein expression in constant light.

'Phospho-dawn': most rhythmic phosphopeptides peak in the subjective morning

Analysis of the number of phosphopeptides that peak at each time point revealed that 45% (dataset I) and 73% (dataset II) of rhythmic phosphopeptides peak around subjective dawn in the WT (Figure 4A, Figure 5A,B). This is in agreement with previous observations in

bioRxiv preprint doi: https://doi.org/10.1101/760892; this version posted April 25, 2021. The copyright holder for this preprint (which was not certified by peer review) is the author/funder, who has granted bioRxiv a license to display the preprint in perpetuity. It is made available under aCC-BY-NC-ND 4.0 International license.

Ostreococcus and *Arabidopsis* (9,43). By contrast, in the global proteomics dataset no tendency for increased abundance at dawn was observed (Figure 4C, Figure 5C,D). These observations hold true when using an alternative ANOVA analysis, detecting change rather than rhythmicity, with a p-value cutoff of $p<0.05$ (Figure S 1). Therefore, the preponderance of 'phospho dawn' patterns is more likely due to (de)phosphorylation events rather than to changes in the abundance of the cognate proteins.

Interestingly, almost all of the few phosphopeptides with JTK_CYCLE p-value < 0.05 also peaked at subjective dawn in the CCA1-OX plants (Figure 4B, Figure 5A,B, Figure S 1), which suggests residual rhythmicity phased similarly to the WT. To expand the search for rhythms in the CCA1-OX, we tested whether there are rhythmic phosphopeptides with shorter periods that would have been excluded from the analysis above. We repeated the JTK_CYCLE analysis, allowing periods down to 12 h. Hardly any phosphopeptides had periods of less than 22 h in the WT, while the majority of phosphopeptides had a predicted period of 12 or 16 h in the CCA1-OX (Figure 5E,F). Interestingly, the majority of those short-period rhythmic phosphopeptides also peaked at 24 h or 48 h (Figure 5A,B). In conclusion, in both of our independent WT phosphoproteomics datasets, the majority of phosphopeptides peak around subjective dawn, and this 'phospho dawn' may not be completely abolished by disruption of the TTFL.

Kinase prediction suggests CDPK/SnRK family members target dawn phased phosphopeptides

We reasoned that there may be a kinase activity that is present predominantly around subjective dawn which is either very robustly dawn-timed by the TTFL even when it is strongly impaired, or an alternative oscillator, such as an NTO, contributes to the dawn phased kinase activity. Characterisation of the phospho-dawn peptides could help to identify either a very robust dawn-phased TTFL output, or potentially consequences of an NTO. For this reason, we focused on the dawn peaking phosphopeptides to identify candidate kinases, using phosphosite motif analysis and kinase prediction. In these analyses we used the ZT24 or

bioRxiv preprint doi: https://doi.org/10.1101/760892; this version posted April 25, 2021. The copyright holder for this preprint (which was not certified by peer review) is the author/funder, who has granted bioRxiv a license to display the preprint in perpetuity. It is made available under aCC-BY-NC-ND 4.0 International license.

ZT48 peaking rhythmic (JTK_CYCLE p-value <0.05) phosphopeptides as foreground and all other identified phosphopeptides as background. No target site motifs were significantly over-represented in a consistent way between datasets (Figure S 2, Figure S 3). For predicting candidate kinases, we searched for enrichment of kinase groups that target phosphopeptides with JTK_CYCLE p-value <0.05 (Table 3) using the GPS3 resource. In the WT, both datasets share enrichment of CMGC kinase groups such as MAPK, and CAMK groups. The latter caught our attention since it is the only consistently enriched group in both genotypes and both datasets. The CAMK group was also consistently enriched among significantly changing phosphopeptides scored using ANOVA p-value < 0.05 (Table S 2).

The CAMK group in plants contains the CDPK/SnRK family of kinases with 89 members (44) in the EKPD database (45) that informs GPS3. Interestingly, among the phospho dawn peptides we found phosphosites that may be direct or indirect SnRK1 target proteins according to two proteomics studies (46,47): NITRATE REDUCTASE (NIA) 1 and 2 and the bifunctional enzyme F2KP (Figure S 4, Table S 3). Interestingly, nitrate reductases have been reported as classical SnRK1 targets in other species (48). In light-dark cycles, NIA1 and NIA2 protein abundances are rhythmic (25), while in our analysis under constant light NIA1 protein was not detected in the global analysis and NIA2 protein abundance changed significantly (Figure S 4B) but not in phase with the phosphosites, suggestive of regulated (de)phosphorylation. Another indication of increased SnRK1 activity at subjective dawn are rhythms in phosphopeptides and abundance of the protein FCS-LIKE ZINC FINGER (FLZ)6 (Figure S 5): transcriptional up-regulation of *FLZ6* by SnRK1 signalling has previously been shown (49,50). In a datset with WT seedlings in constant light (51), the *FLZ6* transcript peaks 4h before the FLZ6 protein in our dataset.

Rhythmically phosphorylated kinases and phosphatases

Since kinases and phosphatases themselves can be regulated by phosphorylation, we were interested in rhythmic phosphopeptides of kinases and phosphatases. Identification of

bioRxiv preprint doi: https://doi.org/10.1101/760892; this version posted April 25, 2021. The copyright holder for this preprint (which was not certified by peer review) is the author/funder, who has granted bioRxiv a license to display the preprint in perpetuity. It is made available under aCC-BY-NC-ND 4.0 International license.

455 rhythmic kinase or phosphatase activities in the WT could help to discover components of
456 clock output pathways that are mediated *via* protein phosphorylation.
457 For two kinases, CRK8 and AT5G61560, we found rhythmic phosphopeptides in the WT
458 where protein abundance did not oscillate in parallel, indicating that rhythmicity is due to
459 phosphorylation rather than changes in protein abundance (Figure S 6). CRK8 is a member of
460 the CDPK-SnRK1 superfamily (44), To our knowledge no specific functions have been
461 investigated for either of these kinases.
462 All rhythmically phosphorylated phosphatases in our data are members of the protein
463 phosphatase 2C (PP2C) family (Figure S 7) and were classified as rhythmic only in the WT.
464 PP2C G1 (Figure S 7A) is involved in ABA dependent salt stress response and, in contrast to
465 PP2CAs is a positive ABA signalling regulator (52) but to our knowledge, no reports exist on
466 the functional relevance of its own phosphorylation. AT3G51470 is also a PP2C G family
467 member, was only rhythmic in dataset I and no functional information is available (53). The
468 final PP2C POLTERGEIST (POL, Figure S 7C) is involved in stem cell regulation (54). In
469 the CCA1-OX data, the profiles for the kinases and phosphatases discussed above can show
470 some similarity to the WT pattern but none were classified as rhythmic by JTK_CYCLE. The
471 biochemical mechanisms underlying the relatively robust phosphoprotein rhythms in the WT
472 should prove easier to investigate than any remaining rhythmicity in the CCA1-OX.
473
474 *Phospho-null mutation of Ser267 of the enzyme F2KP enhances F6P-2kinase activity in-vitro*
475 As an example of how our datasets can be used to investigate new clock output pathways, we
476 analysed the molecular function of a phosphosite of the bifunctional enzyme F2KP. Several
477 phosphosites were detected in F2KP with only Ser276 showing a circadian rhythm in the WT,
478 in dataset II only but at a very high significance level (Figure S 4C, Supplementary Data S3).
479 One F2KP peptide was detected in the global protein analysis of dataset II. Its changes over
480 the timecourse are not significant and do not parallel the Ser276 phosphopeptide, therefore it
481 is unlikely that the rhythm in Ser276 phosphorylation is caused by changes in F2KP protein
482 abundance.

bioRxiv preprint doi: https://doi.org/10.1101/760892; this version posted April 25, 2021. The copyright holder for this preprint (which was not certified by peer review) is the author/funder, who has granted bioRxiv a license to display the preprint in perpetuity. It is made available under aCC-BY-NC-ND 4.0 International license.

We tested whether the Ser276 phosphorylation site is relevant for F2KP function, since this site is highly conserved with other plant species (Figure S 8A), and a very specific enzymatic assay has been described (41,55). Maximum F6P,2K activity was measured of GST-tagged phosphomimetic mutants S276D and S276A, and the unmutated WT control enzyme *in vitro*. Two independent preparations (bacterial expression and purification using a GST tag) were tested to ensure reproducibility. Equivalence of the amounts of expressed F2KP protein in assays was verified by western blotting with two different antibodies (Figure 6C, Figure S 8D). S276A had an approximately 2.5 fold increased activity compared to the unmutated version, while S276D had only slightly increased activity (Figure 6 A,B, Figure S 8B,C,E). The rhythmicity observed at this phosphosite is therefore consistent with a rhythmic input to F2KP function in central carbon metabolism.

Discussion

This study focusses on global and phospho-proteomic timeseries in *Arabidopsis* plants harvested under constant light conditions, where rhythmicity is driven by the circadian clock. In WT plants, we tested the prevalence of circadian rhythms in protein phosphorylation and abundance, which has rarely been reported. In the CCA1-OX transgenic line, we tested the importance of the clock gene circuit for that rhythmic regulation, given that markers of a Non-Transcriptional Oscillator (NTO) are rhythmic in Arabidopsis, and that protein phosphorylation drives the best-characterised NTO in cyanobacteria.

Could an NTO contribute to the phospho-dawn?

CCA1-OX transgenic lines have been widely used as an approximation of a plant without a functional clock. In this line we found very few rhythmic phosphopeptides and proteins, and those with statistical significance typically had less convincing waveforms than rhythms in the WT (Table 1). Therefore, if an NTO exists in *Arabidopsis*, it confers rhythmicity only to very few of the phosphosites we detected. Intriguingly, in both datasets, we still observe the

bioRxiv preprint doi: https://doi.org/10.1101/760892; this version posted April 25, 2021. The copyright holder for this preprint (which was not certified by peer review) is the author/funder, who has granted bioRxiv a license to display the preprint in perpetuity. It is made available under aCC-BY-NC-ND 4.0 International license.

phospho-dawn phenomenon in the CCA1-OX (Figure 4, Figure 5, Figure S 1), whereas a uniform phase distribution would be expected in the noise-driven fluctuations of an arrhythmic plant. It remains possible that an NTO controls this fraction of dawn-phased phosphorylation, albeit too weakly to yield robust rhythms, whereas the majority of phosphoprotein rhythmicity requires a functioning clock gene circuit. We cannot exclude that some rhythmicity of that canonical gene circuit remains even in the CCA1-OX, for example as the CaMV 35S promoter does not confer strong expression in all tissues (56). Additional experiments, such as phosphoproteomics in other arrhythmic mutants, testing other post-translational markers such as redox modifications, and identifying NTO outputs other than PRX over-oxidation (19) and Mg^{2+} rhythms (20,21) might further define the effects of a potential NTO in *Arabidopsis*.

Proteins with rhythmic abundance

We found that the proportion of rhythmic phosphopeptides is larger than for protein abundance, but smaller than for rhythmic transcripts (Table 1). The set of rhythmic proteins does not support extensive inference, though we note that the three examples of rhythmic proteins in Figure 2 all follow the rhythmic regulation of their cognate transcripts. MIPS1 (Figure 2A) is transcriptionally induced by light, acting through FAR-RED ELONGATED HYPOCOTYLS (FHY)3 and FAR-RED IMPAIRED RESPONSE (FAR)1 at the transition from darkness to light in light-dark cycles, and enhances myo-inositol abundance, which in turn limits oxidative stress at the onset of photosynthesis (57,58). Rhythmic *MIPS1* transcript abundance peaks towards the end of the subjective night in constant light (59,60), before a protein peak shortly after subjective dawn. The rhythmic control of MIPS1 abundance is consistent with anticipation of light-induced oxidative stress, providing a potential physiological function in addition to the subsequent, light-responsive induction of myo-inositol production.

BAM3 (Figure 2B) is the dominant beta-amylase contributing to starch degradation (61). The circadian clock is key for the timing of night-time starch degradation (62). In light-dark

bioRxiv preprint doi: https://doi.org/10.1101/760892; this version posted April 25, 2021. The copyright holder for this preprint (which was not certified by peer review) is the author/funder, who has granted bioRxiv a license to display the preprint in perpetuity. It is made available under aCC-BY-NC-ND 4.0 International license.

539 cycles, *BAM3* transcript abundance drops at the beginning of the day and increases during the
540 night (63,64), and this pattern persists in constant light (59,60). We observe a protein
541 abundance pattern that matches the transcript dynamics, indicating that the transcriptional
542 control may be responsible for the protein rhythm. This is also the case for LHCB2.2 (Figure
543 2C), a component of the photosystem II light harvesting complex (60).
544
545 *Proteins with newly discovered phosphopeptide rhythms*
546 We show four examples of newly discovered phosphopeptide rhythms in Figure 3. ASN2
547 (Figure 3A) is one out of three described *Arabidopsis* asparagine synthetases which catalyse
548 the transfer of an amino group from glutamine to aspartate, producing asparagine and
549 glutamate, but ASN2 may also directly use ammonia as a substrate (65,66). The two most
550 expressed asparagine synthetase enzymes in Arabidopsis are ASN1 and ASN2 (65), and in
551 contrast to ASN1, the physiological function of ASN2 is less well understood. We did not
552 find any evidence for ASN2 protein abundance rhythms (Figure 3A), indicating that the
553 phosphosite's peak near subjective dawn is due to rhythmic kinase and / or phosphatase
554 action. Interestingly, the ammonia transporter AMT1;1 also has a rhythmic phosphosite with
555 a temporal profile that parallels the ASN2 peptide (Data S3, Table 2). The presence of
556 rhythmic phosphosites of proteins involved in nitrate metabolism or transport in our data and
557 (9) supports the notion that nitrogen related processes are under control of the circadian clock
558 at the post-translational level, in part through rhythmic AMT1;1 and ASN2 phosphorylation.
559
560 In water transport, our results demonstrate a previously undiscovered phosphosite rhythm on
561 the aquaporin PLASMA MEMBRANE INTRINSIC PROTEIN (PIP)2;7 (Figure 3B).
562 According to (67) this phosphosite is a CPK1 and CPK34 target, and its abundance decreases
563 in response to ABA treatment (68). In response to salt stress, the entire protein is internalised
564 from the plasma membrane, with a concomitant reduction in hydraulic conductivity (69),
565 indicating that decreasing PIP2;7 activity limits water loss. Rhythmic phosphorylation of
566 other aquaporins was previous demonstrated in constant light or darkness (9,70). Therefore,

bioRxiv preprint doi: https://doi.org/10.1101/760892; this version posted April 25, 2021. The copyright holder for this preprint (which was not certified by peer review) is the author/funder, who has granted bioRxiv a license to display the preprint in perpetuity. It is made available under aCC-BY-NC-ND 4.0 International license.

PIP2;7 may, together with other aquaporins, mediate circadian clock regulation of hydraulic conductivity or high salinity response through its phosphorylation status.

In carbon transport, a newly discovered phosphosite rhythm was found for the sucrose efflux transporter SWEET12 (Figure 3C) (71). To our knowledge, the function of this phosphosite is unknown but one may speculate that this rhythm could reflect circadian control of carbon reallocation.

Finally, we have high confidence in the rhythmicity of a phosphopeptide of the putative RNA decapping protein VARICOSE RELATED (VCR) (Figure 3D). VCR and its close homologue VARICOSE (VCS) interact with and are phosphorylated by SnRK2.6 and SnRK2.10 at several serines (72,73). While the VCR phosphosite shown in Fig S6D is not one of the phosphosites identified by (73), SnRK2.10 phosphorylates an almost identical site on VCS (TLSYPTPPLNLQpSPR). Therefore, it is very likely that the corresponding site on VRC is also a SnRK2.10 target.

Altogether, these examples demonstrate how our data can be used to generate hypotheses on clock output pathways affecting different aspects of plant physiology through phosphorylation.

A rhythmic F2KP phosphosite is biochemically relevant

The specific roles of most of the rhythmic phosphorylation sites identified in our study have not been investigated. To exemplify in an experimental approach how circadian phosphorylation of a protein can be linked to its function, we analysed the effect of a phosphosite mutation on the activity of the enzyme F2KP. F2KP is one of the regulators of carbon partitioning into starch and sucrose (74) and is necessary to maintain normal growth in fluctuating light conditions (75). With its kinase domain it can synthesize F-2,6-BP from F-6-P, and with its phosphatase domain it catalyzes the reverse reaction (74).

The phosphosite of interest, Ser276, is within the plant-specific regulatory N-terminal domain (42,76) but is not among the phosphosites in the known 14-3-3 binding site (77). Ser276 is regulated by SnRK1 (46) and is conserved in many plant species (Figure S 8A).

bioRxiv preprint doi: https://doi.org/10.1101/760892; this version posted April 25, 2021. The copyright holder for this preprint (which was not certified by peer review) is the author/funder, who has granted bioRxiv a license to display the preprint in perpetuity. It is made available under aCC-BY-NC-ND 4.0 International license.

595 Our *in-vitro* F-6-P,2 kinase activity measurement experiments showed that substitution of
596 Ser276 by Ala increases F2KP's kinase activity. It is unknown whether *in vitro* expressed
597 F2KP is phosphorylated at Ser276 or not. However, comparison of Ser276 mutation to Ala
598 with the WT and with mutation to Asp, suggests that a lack of negative charge at position 276
599 leads to increased kinase activity. In dataset II, pSer276 decreased gradually during the
600 subjective day (Figure S4C). Assuming that the phospho mimic / WT and null mutations
601 reflect the behaviour of the phosphoryated and non-phosphorylated site, respectively, we
602 extrapolate that towards the end of the day, more F-2,6-BP is produced and therefore starch
603 synthesis is favoured over UDP-glucose and sucrose synthesis. Indeed, F-2,6-BP levels in the
604 plant increase slowly across the day in short day conditions (77). Testing the function of these
605 mutations *in planta* will be interesting to determine whether this phosphosite has
606 physiological relevance, in addition to biochemical effectiveness.
607
608 *Phospho-dawn is likely mediated by several different kinases*
609 We aimed to characterise the phospho-dawn phenomenon as it may point to novel dawn-
610 specific circadian clock output through post-translational mechanisms. Although the striking
611 abundance of dawn-phased phosphopeptides could partly be biased towards the easily
612 detectable or abundant phosphopeptides of our dataset, it is consistent with highest transcript
613 expression of kinases and phosphatases at the end of the night in diel time courses (26,78).
614 Our kinase prediction revealed enrichment of some CMGC subgroups, such as MAPK, CK2,
615 GSK, DYRK, CDK or DAPK. CK2 is involved in the circadian clock function in Arabidopsis
616 by phosphorylating CCA1 (4,79). A previous study reported enrichment of predominantly
617 CK2 predictions among significantly changing phosphopeptides (9). Roles for MAPK and
618 GSK have been reported for the circadian clock function in other eukaryotes (80–83).
619 However, the most consistently enriched group of kinases at subjective dawn in our datasets
620 is the CAMK group (Table 3, Table S 2), which comprises the 89 members of the CDPK-
621 SnRK superfamily of kinases.

bioRxiv preprint doi: https://doi.org/10.1101/760892; this version posted April 25, 2021. The copyright holder for this preprint (which was not certified by peer review) is the author/funder, who has granted bioRxiv a license to display the preprint in perpetuity. It is made available under aCC-BY-NC-ND 4.0 International license.

All of these 89 CDPK-SnRK member are potential candidates for causing the observed phospho-dawn. Not all of these kinases have been studied in much detail, and for the majority of rhythmic phosphopeptides no experimental evidence for kinase specificities exists. However, making use of literature on existing kinase – target pairs can help to narrow down candidates. For example, as mentioned above, CPK1, CPK34 and likely SnRK2.10 phosphorylate dawn-peaking phosphosites shown in Figure 3. In addition, SnRK and CPK / CDPK kinases can themselves be regulated by phosphorylation (44). CRK8, of which we found a very prominently dawn-peaking rhythmic phosphopeptide (Figure S 6A), is therefore another candidate phospho-dawn kinase.

We also show that several previously reported SnRK1 regulated sites are rhythmic with peaks around subjective dawn including phosphopeptides of F2KP and nitrate reductases NIA1 and NIA2 (Figure S 4). Additional indication comes from the protein FLZ6 which is transcriptionally induced by and interacts with SnRK1 and may serve as a platform for SnRK1 signalling (84). FLZ6 protein abundance and two phosphopeptides were rhythmic in the WT with a peak around subjective dawn (Figure S 5). SnRK1 may be a particularly relevant candidate as its involvement in circadian timing has previously been reported (85–87) and as it is an important metabolic hub. In normal light-dark conditions the morning is associated with profound metabolic changes in plants, such as the transition from using starch to direct photoassimilates, or to the alternative, a starvation response if light intensities remain low while starch is almost depleted.

SnRK1 signaling is regarded as antagonistic to TOR signaling (47). Nevertheless, RPS6A and RPS6B phosphosites that are targets of the TOR signalling kinase S6K, are rhythmically phosphorylated in the WT, and in dataset I also in the CCA1-OX (Table 2, supplementary data S3 and (9)), with peaks at subjective dawn. This adds to growing evidence that the interplay between SnRK1 and TOR may be more complex than simply antagonistic (88). In fact, the above-mentioned SnRK1 induced FLZ6 negatively feeds back to SnRK1, and this has been suggested as a mechanism to allow sufficient TOR activity in spite of high SnRK1

bioRxiv preprint doi: https://doi.org/10.1101/760892; this version posted April 25, 2021. The copyright holder for this preprint (which was not certified by peer review) is the author/funder, who has granted bioRxiv a license to display the preprint in perpetuity. It is made available under aCC-BY-NC-ND 4.0 International license.

activity (50), which may allow RPS6 phosphorylation to peak at approximately the same time as SnRK1 activity.

Altogether, the identities of the phospho dawn peptides in our study, along with their known and predicted kinases suggest that phospho-dawn is caused not by a single kinase but several members of the SnRK-CDPK family and also potentially kinases outside this family such as S6K. Further experimentation is required to give evidence for involvement of any such kinases in phospho-dawn, such as time courses of kinase activity and time-resolved phosphoproteomics in mutants of specific candidate kinases. Finding mechanisms that connect the canonical oscillator to prominent post-translational changes at dawn could reveal major clock output pathways that may control a wide range of physiological functions and expand our understanding of how the circadian oscillator increases plant fitness.

Acknowledgements

We thank Lisa Imrie, Katalin Kis and Helle K Mogensen for expert technical support.

Funding

This work was supported by the Wellcome Trust [096995/Z/11/Z] and BBSRC, and EPSRC awards [BB/D019621] and [BB/J009423].

Data availability

The data are publicly available in the pep2pro database (31) at http://fgcz-pep2pro.uzh.ch (Assembly names ‘ed.ac.uk Global I’, ‘ed.ac.uk Global II’, ‘ed.ac.uk Phospho I’, ‘ed.ac.uk Phospho II’) and have been deposited to the ProteomeXchange Consortium (http://proteomecentral.proteomexchange.org) via the PRIDE partner repository (32) with the dataset identifier PXD009230. Exported .csv files from Progenesis with all peptide and protein quantifications can be found in the online supplementary material (Data S1 and S2).

bioRxiv preprint doi: https://doi.org/10.1101/760892; this version posted April 25, 2021. The copyright holder for this preprint (which was not certified by peer review) is the author/funder, who has granted bioRxiv a license to display the preprint in perpetuity. It is made available under aCC-BY-NC-ND 4.0 International license.

References

1. Pokhilko, A. *et al.* The clock gene circuit in Arabidopsis includes a repressilator with additional feedback loops. *Mol. Syst. Biol.* **8,** 574 (2012).

2. Fogelmark, K. & Troein, C. Rethinking Transcriptional Activation in the Arabidopsis Circadian Clock. *PLoS Comput. Biol.* **10,** e1003705 (2014).

3. van Ooijen, G. & Millar, A. J. Non-transcriptional oscillators in circadian timekeeping. *Trends Biochem. Sci.* **37,** 484–92 (2012).

4. Daniel, X., Sugano, S. & Tobin, E. M. CK2 phosphorylation of CCA1 is necessary for its circadian oscillator function in Arabidopsis. *Proc. Natl. Acad. Sci. U. S. A.* **101,** 3292–7 (2004).

5. Nishiwaki, T. *et al.* Role of KaiC phosphorylation in the circadian clock system of Synechococcus elongatus PCC 7942. *Proc. Natl. Acad. Sci. U. S. A.* **101,** 13927–13932 (2004).

6. Maier, B. *et al.* A large-scale functional RNAi screen reveals a role for CK2 in the mammalian circadian clock. *Genes Dev.* **23,** 708–718 (2009).

7. Yang, Y., Cheng, P., He, Q., Wang, L. & Liu, Y. Phosphorylation of FREQUENCY protein by casein kinase II is necessary for the function of the Neurospora circadian clock. *Mol. Cell. Biol.* **23,** 6221–8 (2003).

8. Kusakina, J. & Dodd, A. N. Phosphorylation in the plant circadian system. *Trends Plant Sci.* 1–9 (2012). doi:10.1016/j.tplants.2012.06.008

9. Choudhary, M. K., Nomura, Y., Wang, L., Najagami, H. & Somers, D. E. Quantitative circadian phosphoproteomic analysis of Arabidopsis reveals extensive clock control of key components in physiological, metabolic and signaling pathways. *Mol. Cell. Proteomics* **14,** 2243–2260 (2015).

10. Leloup, J. C. & Goldbeter, A. Toward a detailed computational model for the mammalian circadian clock. *Proc Natl Acad Sci U S A* **100,** 7051–7056 (2003).

11. Baker, C. L., Loros, J. J. & Dunlap, J. C. The circadian clock of Neurospora crassa. *FEMS Microbiol. Rev.* **36,** 95–110 (2012).

12. Takahashi, J. S. Transcriptional architecture of the mammalian circadian clock. *Nat. Rev. Genet.* (2016). doi:10.1038/nrg.2016.150

13. Mauvoisin, D. *et al.* Circadian clock-dependent and -independent rhythmic proteomes implement distinct diurnal functions in mouse liver. *Proc. Natl. Acad. Sci. U. S. A.* (2013). doi:10.1073/pnas.1314066111

14. Lück, S., Thurley, K., Thaben, P. F. & Westermark, P. O. Rhythmic Degradation Explains and Unifies Circadian Transcriptome and Proteome Data. *Cell Rep.* 741–751 (2014). doi:10.1016/j.celrep.2014.09.021

15. Choudhary, M. K., Nomura, Y., Shi, H., Nakagami, H. & Somers, D. E. Circadian Profiling of

bioRxiv preprint doi: https://doi.org/10.1101/760892; this version posted April 25, 2021. The copyright holder for this preprint (which was not certified by peer review) is the author/funder, who has granted bioRxiv a license to display the preprint in perpetuity. It is made available under aCC-BY-NC-ND 4.0 International license.

the Arabidopsis Proteome Using 2D-DIGE. *Front. Plant Sci.* **7,** 1–14 (2016).

16. Nakajima, M. *et al.* Reconstitution of circadian oscillation of cyanobacterial KaiC phosphorylation in vitro. *Science* **308,** 414–5 (2005).

17. O'Neill, J. S. *et al.* Circadian rhythms persist without transcription in a eukaryote. *Nature* **469,** 554–558 (2011).

18. Neill, J. S. O. & Reddy, A. B. Circadian clocks in human red blood cells. *Nature* **469,** 498–503 (2011).

19. Edgar, R. S. *et al.* Peroxiredoxins are conserved markers of circadian rhythms. *Nature* **485,** 459–464 (2012).

20. Feeney, K. A. *et al.* Daily magnesium fluxes regulate cellular timekeeping and energy balance. *Nature* **532,** 375–379 (2016).

21. Henslee, E. A. *et al.* Rhythmic potassium transport regulates the circadian clock in human red blood cells. *Nat. Commun.* **8,** (2017).

22. Reddy, A. B. *et al.* Circadian orchestration of the hepatic proteome. *Curr. Biol.* **16,** 1107–15 (2006).

23. Robles, M. S., Cox, J. & Mann, M. In-Vivo Quantitative Proteomics Reveals a Key Contribution of Post-Transcriptional Mechanisms to the Circadian Regulation of Liver Metabolism. *PLoS Genet.* **10,** (2014).

24. Robles, M. S. *et al.* Phosphorylation Is a Central Mechanism for Circadian Control of Metabolism and Physiology. *Cell Metab.* **0,** 35–48 (2016).

25. Uhrig, R. G. *et al.* Diurnal dynamics of the Arabidopsis rosette proteome and phosphoproteome. *Plant Cell Environ.* 821–841 (2020). doi:10.1111/pce.13969

26. Uhrig, R. G., Schläpfer, P., Roschitzki, B., Hirsch-Hoffmann, M. & Gruissem, W. Diurnal changes in concerted plant protein phosphorylation and acetylation in Arabidopsis organs and seedlings. *Plant J.* **99,** 176–194 (2019).

27. Wang, Z. Y. & Tobin, E. M. Constitutive expression of the CIRCADIAN CLOCK ASSOCIATED 1 (CCA1) gene disrupts circadian rhythms and suppresses its own expression. *Cell* **93,** 1207–17 (1998).

28. Krahmer, J., Hindle, M. M., Martin, S. F., Bihan, T. Le & Millar, A. J. in *Circadian Rhythm. Biol. Clocks* **551,** 405–431 (Elsevier Inc., 2015).

29. Elias, J. E. & Gygi, S. P. Target-Decoy Search Strategy for Mass. *Methods Mol. Biol.* **604,** 55–71 (2010).

30. Hindle, M. M. *et al.* qpMerge: Merging different peptide isoforms using a motif centric strategy. *bioRxiv* **047100,** (2016).

31. Baerenfaller, K. *et al.* pep2pro: a new tool for comprehensive proteome data analysis to reveal

bioRxiv preprint doi: https://doi.org/10.1101/760892; this version posted April 25, 2021. The copyright holder for this preprint (which was not certified by peer review) is the author/funder, who has granted bioRxiv a license to display the preprint in perpetuity. It is made available under aCC-BY-NC-ND 4.0 International license.

information about organ-specific proteomes in Arabidopsis thaliana. *Integr. Biol. (Camb).* **3,** 225–37 (2011).

32. Vizcaíno, J., Deutsch, E. & Wang, R. ProteomeXchange provides globally coordinated proteomics data submission and dissemination. *Nat. Biotechnol.* **32,** 223–226 (2014).

33. R Core Team. R: A Language and Environment for Statistical Computing. (2015). at <http://www.r-project.org/>

34. Suzuki, R. & Shimodaira, H. pvclust: Hierarchical Clustering with P-Values via Multiscale Bootstrap Resampling. (2015). at <http://cran.r-project.org/package=pvclust>

35. Hughes, M. E., Hogenesch, J. B. & Kornacker, K. JTK_CYCLE: An Efficient Nonparametric Algorithm for Detecting Rhythmic Components in Genome-Scale Data Sets. *J. Biol. Rhythms* **25,** 372–380 (2010).

36. Benjamini, Y. & Hochberg, Y. Controlling the False Discovery Rate : A Practical and Powerful Approach to Multiple Testing. *J R Stat. Soc B* **57,** 289–300 (1995).

37. Xue, Y. *et al.* GPS 2.0: Prediction of kinase-specific phosphorylation sites in hierarchy 10.1074/mcp.M700574-MCP200. *Mol Cell Proteomics* M700574--MCP200 (2008). at <http://www.mcponline.org/cgi/content/abstract/M700574-MCP200v1>

38. Liu, Z. *et al.* GPS 3.0: web servers for the prediction of protein post-translational modification sites. *Manuscr. Submitt.* (2015).

39. Alexa, A., Rahnenführer, J. & Lengauer, T. Improved scoring of functional groups from gene expression data by decorrelating GO graph structure. *Bioinformatics* **22,** 1600–7 (2006).

40. Kalt-torres, W., Kerr, P. S., Usuda, H. & Huber, S. C. Diurnal Changes in Maize Leaf Photosynthesis. *Plant Physiol.* **83,** 283–288 (1987).

41. Van Schaftingen, E., Lederer, B., Bartrons, R. & Hers, H.-G. A Kinetic Study of Pyrophosphate : Fructose-6-Phosphate Phosphotransferase from Potato Tubers Application to a Microassay of Fructose 2,6-Bisphosphate. *Eur. J. Biochem.* **129,** 191–195 (1982).

42. Villadsen, D. & Nielsen, T. H. N-terminal truncation affects the kinetics and structure of fructose-6-phosphate 2-kinase/fructose-2,6-bisphosphatase from Arabidopsis thaliana. *Biochem. J.* **359,** 591–7 (2001).

43. Noordally, Z. B. *et al.* Circadian protein regulation in the green lineage I. A phospho-dawn anticipates light onset before proteins peak in daytime. *bioRxiv* (2018). doi:http://dx.doi.org/10.1101/287862

44. Hrabak, E. M. *et al.* The Arabidopsis CDPK-SnRK Superfamily of Protein Kinases. *Plant Physiol.* **132,** 666–680 (2003).

45. Wang, Y. *et al.* EKPD: A hierarchical database of eukaryotic protein kinases and protein phosphatases. *Nucleic Acids Res.* **42,** 496–502 (2014).

bioRxiv preprint doi: https://doi.org/10.1101/760892; this version posted April 25, 2021. The copyright holder for this preprint (which was not certified by peer review) is the author/funder, who has granted bioRxiv a license to display the preprint in perpetuity. It is made available under aCC-BY-NC-ND 4.0 International license.

46. Cho, H. Y., Wen, T. N., Wang, Y. T. & Shih, M. C. Quantitative phosphoproteomics of protein kinase SnRK1 regulated protein phosphorylation in Arabidopsis under submergence. *J. Exp. Bot.* **67,** 2745–2760 (2016).

47. Nukarinen, E. *et al.* Quantitative phosphoproteomics reveals the role of the AMPK plant ortholog SnRK1 as a metabolic master regulator under energy deprivation. *Sci. Rep.* **6,** 31697 (2016).

48. Sugden, C., Donaghy, P. G., Halford, N. G. & Hardie, D. G. Two SNF1-related protein kinases from spinach leaf phosphorylate and inactivate 3-hydroxy-3-methylglutaryl-coenzyme A reductase, nitrate reductase, and sucrose phosphate synthase in vitro. *Plant Physiol* **120,** 257–274 (1999).

49. Jamsheer, M. K. & Laxmi, A. Expression of Arabidopsis FCS-like Zinc finger genes is differentially regulated by sugars, cellular energy level, and abiotic stress. *Front. Plant Sci.* **6,** 1–12 (2015).

50. Jamsheer, M. K. *et al.* The FCS-like zinc finger scaffold of the kinase SnRK1 is formed by the coordinated actions of the FLZ domain and intrinsically disordered regions. *J. Biol. Chem.* **293,** 13134–13150 (2018).

51. Covington, M. F., Maloof, J. N., Straume, M., Kay, S. a & Harmer, S. L. Global transcriptome analysis reveals circadian regulation of key pathways in plant growth and development. *Genome Biol.* **9,** R130 (2008).

52. Liu, X. *et al.* AtPP2CG1, a protein phosphatase 2C, positively regulates salt tolerance of Arabidopsis in abscisic acid-dependent manner. *Biochem. Biophys. Res. Commun.* **422,** 710–715 (2012).

53. Sahoo, S. A., Raghuvanshi, R., Srivastava, A. K. & Suprasanna, P. in *Protein Phosphatases Stress Manag. Plants Funct. Genomic Perspect.* (ed. Pandey, G. K.) 163–201 (Springer International Publishing, 2020). doi:10.1007/978-3-030-48733-1_10

54. Yu, L. P., Miller, A. K. & Clark, S. E. POLTERGEIST encodes a protein phosphatase 2C that regulates CLAVATA pathways controlling stem cell identity at Arabidopsis shoot and flower meristems. *Curr. Biol.* **13,** 179–188 (2003).

55. Kalt-Torres, W. & Huber, S. C. Diurnal Changes in Maize Leaf Photosynthesis. *Plant Physiol.* **83,** 283–288 (1987).

56. Holtorf, S., Apel, K. & Bohlmann, H. Comparison of different constitutive and inducible promoters for the overexpression of transgenes in Arabidopsis thaliana. *Plant Mol. Biol.* **29,** 637–646 (1995).

57. Donahue, J. L. *et al.* The Arabidopsis thaliana myo-inositol 1-phosphate synthase1 gene is required for myo-inositol synthesis and suppression of cell death. *Plant Cell* **22,** 888–903 (2010).

bioRxiv preprint doi: https://doi.org/10.1101/760892; this version posted April 25, 2021. The copyright holder for this preprint (which was not certified by peer review) is the author/funder, who has granted bioRxiv a license to display the preprint in perpetuity. It is made available under aCC-BY-NC-ND 4.0 International license.

58. Ma, L. *et al.* Arabidopsis FHY3 and FAR1 Regulate Light- Induced myo-Inositol Biosynthesis and Oxidative Stress Responses by Transcriptional Activation of MIPS1. *Mol. Plant* **9,** 541–557 (2016).

59. Edwards, K. D. *et al.* FLOWERING LOCUS C Mediates Natural Variation in the High-Temperature Response of the Arabidopsis Circadian Clock. *Plant Cell* **18,** 639–650 (2006).

60. Covington, M. F. & Harmer, S. L. The Circadian Clock Regulates Auxin Signaling and Responses in Arabidopsis. *PLoS Biol.* **5,** 1773–1784 (2007).

61. Monroe, J. D. Involvement of five catalytically active Arabidopsis β-amylases in leaf starch metabolism and plant growth. *Plant Direct* **4,** 1–10 (2020).

62. Graf, A., Schlereth, A., Stitt, M. & Smith, A. M. Circadian control of carbohydrate availability for growth in Arabidopsis plants at night. *Proc. Natl. Acad. Sci. U. S. A.* **107,** 9458–9463 (2010).

63. Smith, S. *et al.* Diurnal changes in the transcriptome encoding enzymes of starch metabolism provide evidence for both transcriptional and posttranscriptional regulation of starch metabolism in arabidopsis leaves. *Plant Physiol.* **136,** 2687–2699 (2004).

64. Bläsing, O. E. *et al.* Sugars and circadian regulation make major contributions to the global regulation of diurnal gene expression in Arabidopsis. *Plant Cell* **17,** 3257–3281 (2005).

65. Coruzzi, G. M. Primary N-assimilation into Amino Acids in Arabidopsis. *Arab. B.* **2,** e0010 (2003).

66. Wong, H. K., Chan, H. K., Coruzzi, G. M. & Lam, H. M. Correlation of ASN2 Gene Expression with Ammonium Metabolism in Arabidopsis. *Plant Physiol.* **134,** 332–338 (2004).

67. Curran, A. *et al.* Calcium-Dependent Protein Kinases from Arabidopsis Show Substrate Specificity Differences in an Analysis of 103 Substrates. *Front. Plant Sci.* **2,** 1–15 (2011).

68. Kline, K. G., Barrett-Wilt, G. a & Sussman, M. R. In planta changes in protein phosphorylation induced by the plant hormone abscisic acid. *Proc. Natl. Acad. Sci. U. S. A.* **107,** 15986–15991 (2010).

69. Pou, A. *et al.* Salinity-mediated transcriptional and post-translational regulation of the Arabidopsis aquaporin PIP2;7. *Plant Mol. Biol.* **92,** 731–744 (2016).

70. Prado, K. *et al.* Oscillating aquaporin phosphorylation and 14-3-3 proteins mediate the circadian regulation of leaf hydraulics. *Plant Cell* **31,** 417–429 (2019).

71. Chen, L.-Q. *et al.* Sucrose Efflux Mediated by SWEET Proteins as a Key Step for Phloem Transport. *Science (80-.).* **335,** 207–211 (2012).

72. Deyholos, M. K. *et al.* Varicose, a WD-domain protein, is required for leaf blade. *Development* **130,** 6577–6588 (2003).

73. Kawa, D. *et al.* SnRK2 protein kinases and mRNA decapping machinery control root

bioRxiv preprint doi: https://doi.org/10.1101/760892; this version posted April 25, 2021. The copyright holder for this preprint (which was not certified by peer review) is the author/funder, who has granted bioRxiv a license to display the preprint in perpetuity. It is made available under aCC-BY-NC-ND 4.0 International license.

development and response to salt. *Plant Physiol.* **182,** 361–371 (2020).

74. Nielsen, T. H., Rung, J. H. & Villadsen, D. Fructose-2,6-bisphosphate: a traffic signal in plant metabolism. *Trends Plant Sci.* **9,** 556–63 (2004).

75. McCormick, A. J. & Kruger, N. J. Lack of fructose 2,6-bisphosphate compromises photosynthesis and growth in Arabidopsis in fluctuating environments. *Plant J.* **81,** 670–683 (2015).

76. Villadsen, D., Rung, J. H., Draborg, H. & Nielsen, T. H. Structure and heterologous expression of a gene encoding fructose-6-phosphate,2-kinase/fructose-2,6-bisphosphatase from Arabidopsis thaliana. *Biochim. Biophys. Acta* **1492,** 406–413 (2000).

77. Kulma, A. *et al.* Phosphorylation and 14-3-3 binding of Arabidopsis 6-phosphofructo-2-kinase/fructose-2,6-bisphosphatase. *Plant J.* **37,** 654–667 (2004).

78. Bläsing, O. E. *et al.* Sugars and Circadian Regulation Make Major Contributions to the Global Regulation of Diurnal Gene Expression in Arabidopsis. *Plant Cell* **17,** 3257–3281 (2005).

79. Sugano, S., Andronis, C., Ong, M. S., Green, R. M. & Tobin, E. M. The protein kinase CK2 is involved in regulation of circadian rhythms in Arabidopsis. *Proc. Natl. Acad. Sci. U. S. A.* **96,** 12362–6 (1999).

80. Akashi, M. & Nishida, E. Involvement of the MAP kinase cascade in resetting of the mammalian circadian clock. *Genes Dev.* **14,** 645–649 (2000).

81. Iitaka, C., Miyazaki, K., Akaike, T. & Ishida, N. A role for glycogen synthase kinase-3beta in the mammalian circadian clock. *J. Biol. Chem.* **280,** 29397–29402 (2005).

82. Besing, R. C. *et al.* Circadian Rhythmicity of Active GSK3 Isoforms Modulates Molecular Clock Gene Rhythms in the Suprachiasmatic Nucleus. *J. Biol. Rhythms* **XX,** 1–6 (2015).

83. Martinek, S., Inonog, S., Manoukian, A. S. & Young, M. W. A role for the segment polarity gene shaggy/GSK-3 in the Drosophila circadian clock. *Cell* **105,** 769–779 (2001).

84. Nietzsche, M., Schießl, I. & Börnke, F. The complex becomes more complex: protein-protein interactions of SnRK1 with DUF581 family proteins provide a framework for cell- and stimulus type-specific SnRK1 signaling in plants. *Front. Plant Sci.* **5,** 54 (2014).

85. Shin, J. *et al.* The metabolic sensor AKIN10 modulates the Arabidopsis circadian clock in a light-dependent manner. *Plant. Cell Environ.* (2017). doi:10.1111/pce.12903

86. Sánchez-Villarreal, A., Davis, A. M. & Davis, S. J. AKIN10 activity as a cellular link between metabolism and circadian-clock entrainment in Arabidopsis thaliana. *Plant Signal. Behav.* **13,** e1411448 (2018).

87. Frank, A. *et al.* Circadian Entrainment in Arabidopsis by the Sugar-Responsive Transcription Factor bZIP63. *Curr. Biol.* **28,** 2597-2606.e6 (2018).

88. González, A., Hall, M. N., Lin, S. C. & Hardie, D. G. AMPK and TOR: The Yin and Yang of

bioRxiv preprint doi: https://doi.org/10.1101/760892; this version posted April 25, 2021. The copyright holder for this preprint (which was not certified by peer review) is the author/funder, who has granted bioRxiv a license to display the preprint in perpetuity. It is made available under aCC-BY-NC-ND 4.0 International license.

Cellular Nutrient Sensing and Growth Control. *Cell Metab.* **31,** 472–492 (2020).

Footnotes

This work was supported by the Wellcome Trust [096995/Z/11/Z] and BBSRC, and EPSRC awards [BB/D019621] and [BB/J009423].

bioRxiv preprint doi: https://doi.org/10.1101/760892; this version posted April 25, 2021. The copyright holder for this preprint (which was not certified by peer review) is the author/funder, who has granted bioRxiv a license to display the preprint in perpetuity. It is made available under aCC-BY-NC-ND 4.0 International license.

Figure legends

Figure 1: Experiment workflow and comparison of protein and phosphopeptide numbers with published transcriptome time courses. A) WT and CCA1-OX plants were grown in 12h light:12h dark cycles for 22 days and then subjected to continuous light. In dataset I, rosettes were harvested every 4h from ZT12, in dataset II from ZT24 until ZT48 (black arrows) with an additional WT time point at ZT52 (grey arrow). B) Sample processing and data analysis workflow: Plants were crushed and protein was extracted, precipitated and digested in-solution. Peptides were split into 10µg for global protein analysis (of which 4µg were injected) and 490µg for phosphopeptide enrichment on TiO_2 spin tips. Peptides were analysed by LC-MS/MS. Outliers were removed before further bioinformatics analysis. C) Venn diagrams showing overlap of quantified (C,E) and rhythmic (WT only; D,F) transcripts (Covington et al. 2008), proteins and phosphoproteins in dataset I (C,D) and dataset II (E,F).

Figure 2: Examples of three proteins with rhythmic abundance in both datasets. (A) MIPS1, (B) BAM3, (C) LHCB2.2. JTK_CYCLE p-values are indicated under the graphs.

Figure 3: Examples of newly described phosphopeptide rhythms with JTK_CYCLE $p<0.05$ in both datasets. Phosphopeptide from (A) an asparagine synthetase, ASN2, with global protein abundance plots (B) from aquaporin PIP2;7 with global protein abundance plot from dataset I (not detected in dataset II) (C) from the sucrose efflux protein SWEET12 and (D) from VCR. Protein not detected in global proteomics for (C) and (D). JTK_CYCLE p-values are indicated under the graphs.

Figure 4: Whole-dataset protein and phosphopeptide dynamics. Heatmaps were generated by hierarchical clustering of phosphopeptide (A, B) or global protein (C, D) abundance time courses in dataset I and II (indicated on the right) for WT (A,C) and CCA1-OX (B,D).

bioRxiv preprint doi: https://doi.org/10.1101/760892; this version posted April 25, 2021. The copyright holder for this preprint (which was not certified by peer review) is the author/funder, who has granted bioRxiv a license to display the preprint in perpetuity. It is made available under aCC-BY-NC-ND 4.0 International license.

Figure 5: Peak time and period distribution of phosphopeptide and global protein time courses. (A-D): Number of rhythmic (JTK_CYCLE p-value <0.05) phosphopeptides (A,B) or proteins (C,D) peaking at each time point, allowing a period of around 24h (22 to 26) or 12 to 20h. (E-F) Periods according to JTK_CYCLE allowing periods from 12 to 24h for phosphoproteomics dataset I (E) and II (F). Number of rhythmic phosphopeptides (JTK_CYCLE p-value < 0.05) for each predicted period is plotted.

Figure 6: *In vitro* GST-F2KP activity assay with WT and Ser276 point mutations. A) fructose-2,6-bisphosphate (F26BP)) accumulation during the reaction. B) Kinase activity calculated from slopes in (A). C) relative quantification of GST-F2KP in eluates probed with rabbit (Rb) anti F2KP and mouse (Ms) anti GST. Protein blot is shown below quantification for rabbit anti F2KP. A dilution series of a sample mix was used for quantification, ranging from 0.5 to 1.5 loading equivalent of the samples. Averages of both dilution curves were used. Error bars: SEM. * p-value < 0.05 in t-test.

bioRxiv preprint doi: https://doi.org/10.1101/760892; this version posted April 25, 2021. The copyright holder for this preprint (which was not certified by peer review) is the author/funder, who has granted bioRxiv a license to display the preprint in perpetuity. It is made available under aCC-BY-NC-ND 4.0 International license.

Tables

Table 1: Identification counts for global and phosphoproteomics datasets. A) Numbers of quantified and changing identifications in each dataset, B) shared and added numbers of both datasets. In B) protein IDs of peptides are used for simplicity of comparison.

A

	Dataset I				Dataset II			
	Global Proteomics		Phosphoproteomics		Global Proteomics		Phosphoproteomics	
	WT	CCA1-OX	WT	CCA1-OX	WT	CCA1-OX	WT	CCA1-OX
Quantifiable identifications before merging	1896 proteins		2287 phosphopeptides		1340 proteins		1664 phosphopeptides	
Quantifiable identifications after merging			1498 from 944 proteins				1132 from 747 proteins	
Significantly changing (ANOVA p<0.05)	245	147	406	296	68	46	88	83
Adjusted for multiple testing (ANOVA q<0.05)	13	3	56	4	3	2	14	7
Rhythmic by JTK_CYCLE (p<0.05)	171	122	606 from 481 proteins	37 from 32 proteins	45	57	100 from 91 proteins	17 from 17 proteins
Adjusted for multiple testing (JTK:CYCLE q<0.05)	6	0	338	2	6	0	26	0
JTK_CYCLE p<0.05 in both genotypes	17		22		9		3	

B

	Global Proteomics		Phosphoproteomics	
	WT	CCA1-OX	WT	CCA1-OX
JTK p<0.05 detected in both datasets	6	3	48	2
all quantified protein IDs detected in both datasets	137		626	
sum of all quantifiable protein IDs in both datasets	2501		1065	

bioRxiv preprint doi: https://doi.org/10.1101/760892; this version posted April 25, 2021. The copyright holder for this preprint (which was not certified by peer review) is the author/funder, who has granted bioRxiv a license to display the preprint in perpetuity. It is made available under aCC-BY-NC-ND 4.0 International license.

Table 2: List of all proteins and phosphopeptides that are rhythmic in WT or CCA1-OX in both datasets (i.e. shared rhythmic IDs). All p-values are based on JTK_CYCLE analysis. * in some phosphopeptides, the location of phosphorylated residues differs slightly (either shifted by 1-2 residues or one of several phosphates is missing) between datasets, in which case the phosphorylated residues of both datasets are noted (dataset I / dataset II). Bold: phase difference of peak is up to 4h. fam. = family, pr. = protein

A) Phosphopeptides, WT

Accession	Description	Peptide ID dataset I	Peptide ID dataset II	Peptide sequence	Phospho residue(s)	p-value dataset I	p-value dataset II	q-value dataset I	q-value dataset II	Peak dataset I (h)	Peak dataset II (h)
AT4G32340	TPR-like superfam. pr.	15668	12823	SASSLDLNLR	3	9.5E-05	1.9E-09	5.7E-03	2.1E-06	**12**	**32**
AT2G33830	Dormancy/auxin associated fam. pr.	6246	2709	TVAAVAGSPGT PTTPGSAR	13 / 11	2.0E-02	2.0E-08	6.5E-02	8.9E-06	**12**	**40**
AT4G31700	RPS6A	8624	778	SRLSSAAAKPSVTA	1,4,5/1,4,11	2.0E-06	2.4E-08	4.9E-04	8.9E-06	**24**	**24**
AT3G47470	CAB4	715	636	DLSFTSIGSSAK	3	1.3E-06	1.6E-07	4.9E-04	3.0E-05	**28**	**32**
AT3G07650	COL9	8182	11184	AGEAYDYDPLTPT RSY	15	3.0E-03	2.4E-07	2.7E-02	3.8E-05	24	40
AT4G31700	RPS6A	8624	1785	SRLSSAAAKPSVTA	1, 4, 5	2.0E-06	2.8E-07	4.9E-04	3.9E-05	**24**	**24**
AT5G10360	RPS6B	41, 1736	28	SRLSSAPAKPVAA	4 / 1, 4	7.4E-03	4.8E-07	4.0E-02	5.9E-05	32	24
AT4G31700	RPS6A	8624	21	SRLSSAAAKPSVTA	1, 4, 5 / 1, 4	2.0E-06	9.5E-07	4.9E-04	1.1E-04	**24**	**24**
AT5G48250	B-box type zinc finger	11033	16261	SGEAYDYDPMSPT RSY	15 / 16	7.4E-03	1.6E-06	4.0E-02	1.6E-04	24	40
AT1G69870	NRT1.7	7142	8476	ISSPGSILDAEK	3	1.7E-04	3.0E-06	6.8E-03	2.8E-04	**24**	**48**
AT5G40890	CLC-A	1783	1852	HRTLSSTPLALVGAK	3, 5	5.1E-05	1.1E-04	4.0E-03	7.3E-03	**24**	**24**
AT5G53420	CCT motif family pr.	1950	1997	LGAGLVQSPLDR	8	6.0E-03	1.1E-04	3.6E-02	7.3E-03	**28**	**48**
AT5G20670	DUF1677	4202	5127	TSSSGALPGIDGVESR	3 / 4	1.9E-03	1.6E-04	2.3E-02	1.0E-02	**28**	**48**
AT1G73980	Phosphoribulokinase / Uridine kinase fam.	10001	8639	LSLDDDTVSSPK	10	1.7E-02	1.9E-04	5.9E-02	1.1E-02	**28**	**24**
AT1G78020	DUF581	10297, 1700	3249, 1093	LLSMVTPR	3	1.3E-05	2.1E-04	1.5E-03	1.2E-02	**24**	**24**
AT1G78020	DUF581	2081, 5542, 5542	2113, 737, 2081	RHSGDFSDAGHFLR	3	2.4E-02	1.5E-03	7.4E-02	6.2E-02	**24**	**24**
AT1G11310	MLO2	1496	3909	SVENYPSSPSPR	7 / 8, 10	2.3E-04	1.9E-03	7.7E-03	6.9E-02	32	24
AT4G31700	RPS6A	2489	3985	LSSAAAKPSVTA	9	1.5E-03	3.6E-03	2.1E-02	1.2E-01	32	48
AT2G32240	unknown	5883	7383	DIDLSFSSPTKR	8	1.1E-02	4.0E-03	4.9E-02	1.3E-01	**24**	**48**
AT3G13290	VCR	4140	6826	TLSYPTPPLNPQSPR	13	3.0E-03	5.4E-03	2.7E-02	1.6E-01	**28**	**48**
AT4G35100	PIP3A	140	214	ALGSFRSNATN	4, 7	1.1E-02	8.0E-03	4.9E-02	1.9E-01	**28**	**24**
AT5G38640	NagB/RpiA/CoA transferase-like superfam. pr.	4683	1690	DFPDGSTTASPGR	10	6.0E-03	8.8E-03	3.6E-02	2.0E-01	32	24
AT1G37130	NIA2	4382	2045, 2045	VHDDDEDVSSEDE NETHNSNAVYYK	9, 10	9.0E-04	8.8E-03	1.7E-02	2.0E-01	**28**	**28**
AT3G13530	MAPKKK7	3515	6312	SKLPLVGVSSFR	10	3.0E-03	8.8E-03	2.7E-02	2.0E-01	28	40
AT1G35580	CINV1	903	1066	SVLDTPLSSAR	5, 8	1.7E-02	9.7E-03	5.9E-02	2.1E-01	**24**	**24**
AT1G74780	Major Facilitator Superfam. pr.	6279	4702, 5728	TVPHDYSPLISSPK	12	3.0E-03	9.7E-03	2.7E-02	2.1E-01	**28**	**48**
AT3G27700	zinc finger fam. pr.	9563	9073	LDTASDSGAAIASPK	13	4.8E-03	1.1E-02	3.4E-02	2.2E-01	**28**	**48**
AT5G65010	ASN2	4975	4842	AGSDLVDPLPK	3	6.9E-04	1.3E-02	1.6E-02	2.4E-01	**28**	**24**
AT4G31160	DCAF1, DDB1-CUL4 associated factor 1	8754	7154, 8583	VHEGAPDTEVLL ASPR	14	3.5E-02	1.3E-02	9.3E-02	2.4E-01	**28**	**48**
AT4G13510	AMT1;1	214	110	SPSPSGANTTPTPV	1	3.5E-02	1.4E-02	9.3E-02	2.5E-01	32	48
AT5G23660	SWEET12	14806	17187	LGTLTSPEPVAITVVR	6	9.1E-03	1.8E-02	4.3E-02	3.0E-01	24	40
AT3G26730	RING/U-box superfam. pr.	5794	6017	NQTQSLSPPDVSR	7	1.3E-04	2.2E-02	6.2E-03	3.5E-01	**24**	**24**
AT4G20910	HEN1	15648	13859, 13859	SSSPNVFAAPPILQK	3 / 2, 3	9.5E-05	2.6E-02	5.7E-03	3.7E-01	**28**	**24**
AT2G07360	SH3 domain-containing pr.	2769, 5085	9464, 8286	YQSTYEGYGSPIREEP PPPYSYSEPQSR	10	1.1E-02	2.6E-02	4.9E-02	3.7E-01	24	36
AT4G26130	unknown pr.	5416, 7652, 1518	7456	TTSIGDGGEEGVDDK ASNFINK(FK)	3	1.4E-02	2.6E-02	5.3E-02	3.7E-01	24	40
AT1G44800	nodulin MtN21	7377	34568	SQELPITNVVK	1	4.4E-06	2.6E-02	6.5E-04	3.7E-01	**28**	**52**
AT2G46920	POL	7848	11608	SNFSAPLSFR	8	1.9E-03	3.1E-02	2.3E-02	4.1E-01	28	40
AT2G42600	PPC2	1672, 57	62, 40, 4070	MASIDAQLR	3	7.4E-03	4.0E-02	4.0E-02	4.7E-01	32	24
AT3G60240	EIF4G	1585	1579	QVLQGPSATVNSPR	12	3.8E-03	4.3E-02	3.0E-02	4.9E-01	**28**	**48**
AT1G70770	DUF2359	514	169, 800	MTAIDSDDDGVVR	6	7.4E-03	4.3E-02	4.0E-02	4.9E-01	**24**	**48**
AT5G40890	CLC-A	749	406	TLSSTPLALVGAK	3	1.3E-04	4.3E-02	6.2E-03	4.9E-01	**28**	**48**
AT4G12770	Chaperone DnaJ-domain superfam. pr.	238, 238	318	FENVFSSISSSPTK	11	6.0E-03	4.7E-02	3.6E-02	5.2E-01	**28**	**48**

Table 2 *continued*

bioRxiv preprint doi: https://doi.org/10.1101/760892; this version posted April 25, 2021. The copyright holder for this preprint (which was not certified by peer review) is the author/funder, who has granted bioRxiv a license to display the preprint in perpetuity. It is made available under aCC-BY-NC-ND 4.0 International license.

B) Phosphopeptides, CCA1-OX

Accession	Description	Peptide ID dataset I	Peptide ID dataset II	Peptide sequence	Phospho residue(s)	p-value dataset I	p-value dataset II	q-value dataset I	q-value dataset II	Peak dataset I (h)	Peak dataset II (h)
AT2G33830	Dormancy/auxin associated fam. pr.	1348, 43281	2709	TVAAVAGSPGTPTTPGSAR	11	0.023	0.0069	1	1	12	24
AT1G51805	Leucine-rich repeat protein kinase fam. pr.	2617	2514, 1136	VEGTLPSYMQASDGRSPR	16	0.019	0.021	1	1	**24**	**24**

C) Phosphopeptides, CCA1-OX, allowing periods of 12 to 20h

Accession	Description	Peptide ID dataset I	Peptide ID dataset II	Peptide sequence	Phospho residue(s)	p-value dataset I	p-value dataset II	q-value dataset I	q-value dataset II	Peak dataset I (h)	Peak dataset II (h)
AT1G77760	NIA1	4776	1968	SVSSPFMNTASK	3	0.013	0.00067	0.42	0.25	**24**	**48**
AT2G45820	Remorin fam. pr.	1234, 5319	698, 2343	ALAVVEKPIEEHTPK	13	0.019	0.0045	0.42	0.68	**24**	**24**

D) Global proteomics, WT

Accession	Description	p-value dataset I	p-value dataset II	q-value dataset I	q-value dataset II	Peak dataset I (h)	Peak dataset II (h)
AT4G39800	MI-1-P SYNTHASE	6.22E-06	8.7E-12	0.00588435	5.78E-09	**28**	**24**
AT4G17090	BAM3	0.005602	4.6E-05	0.225379284	0.015428	**20**	**44**
AT5G13630	GUN5	0.030091	0.0001	0.427829153	0.027626	**32**	**52**
AT1G78570	RHM1	0.00045	0.00059	0.070946877	0.087173	**28**	**48**
AT1G15820	LHCB6	0.043966	0.02293	0.516391687	0.926734	**12**	**36**
AT4G27440	PORB	0.000255	0.0297	0.06492429	1	**12**	**36**

E) Global proteomics, CCA1-OX

Accession	Description	p-value dataset I	p-value dataset II	q-value dataset I	q-value dataset II	Peak dataset I (h)	Peak dataset II (h)
AT3G47070	unknown	0.034204	0.01201	0.634454201	0.909654	**20**	**40**
AT3G49190	O-acyltransferase fam. pr.	0.001556	0.02209	0.24526271	0.916547	32	44
AT4G39800	MI-1-P SYNTHASE	0.000373	0.03406	0.175519785	0.98762	**24**	**24**

bioRxiv preprint doi: https://doi.org/10.1101/760892; this version posted April 25, 2021. The copyright holder for this preprint (which was not certified by peer review) is the author/funder, who has granted bioRxiv a license to display the preprint in perpetuity. It is made available under aCC-BY-NC-ND 4.0 International license.

Table 3: Summary of GPS3 kinase prediction followed by Fisher's Exact test. Fisher's exact test p-values for enrichment of each kinase group are shown. a) dataset I, b) dataset II. Foreground groups were chosen with JTK_CYCLE p-values <0.05 and peaks or troughs at indicated ZTs.

A) dataset I

	WT, 22 to 26h period				CCA1-OX, 22 to 26h period			CCA1-OX, 12 to 20h period
	peak		trough	all p<0.05	peak	trough	all p<0.05	peak
time point	24h	28h	12h		24h	12h		24h
AGC					0.043			
AGC/NDR		0.0072						
Atypical/TAF1	6.50E-06		2.50E-06					
CAMK		0.0012		0.0040		0.00063	0.0090	0.024
CAMK/DAPK								0.029
CMGC/CK2	0.0012		4.70E-06					
CMGC/MAPK				0.027				
Other / ULK			0.040			0.0030	0.0066	
Other/WNK								0.044

B) dataset II

	WT, 22 to 26h period			CCA1-OX, 22 to 26h period		CCA1-OX, 12 to 20h period
	peak		all p<0.05	peak	all p<0.05	peak
time point	24h	48h		24h		24h
AGC	1.4E-06					
AGC/PDK1	0.0049					
CAMK	0.00024		0.0049			0.048
CAMK-L						0.0035
CAMK-Unique	0.057					
CMGC	0.0061			0.040		
CMGC/GSK	0.0078					
CMGC/MAPK		0.040				
Other/PEK				0.028	0.047	
STE/STE7	0.037					

bioRxiv preprint doi: https://doi.org/10.1101/760892; this version posted April 25, 2021. The copyright holder for this preprint (which was not certified by peer review) is the author/funder, who has granted bioRxiv a license to display the preprint in perpetuity. It is made available under aCC-BY-NC-ND 4.0 International license.

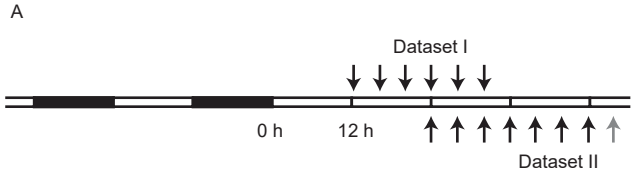

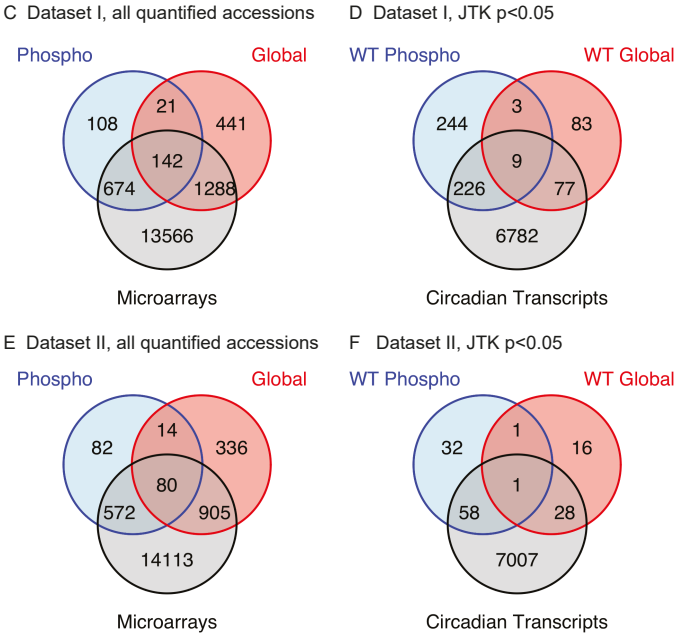

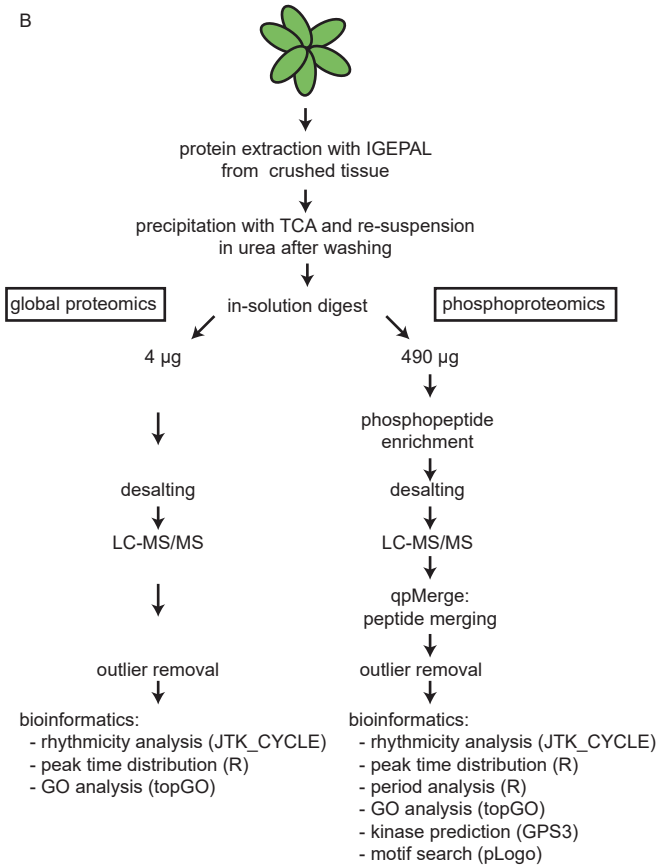

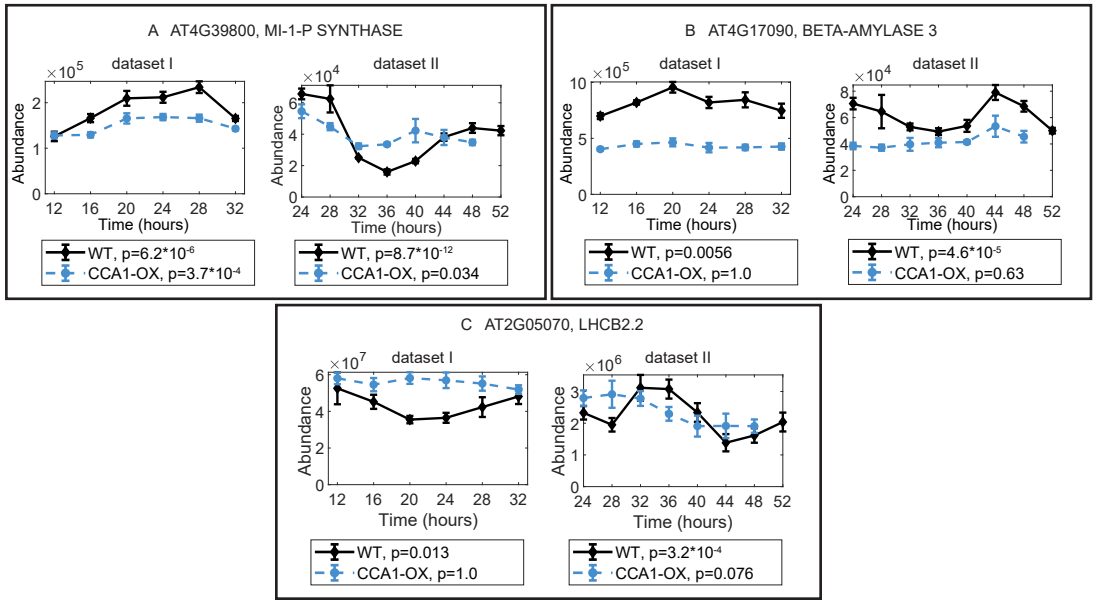
A AT4G39800, MI-1-P SYNTHASE
dataset I
×10^5
Abundance
Time (hours)
WT, p=6.2*10^-6
CCA1-OX, p=3.7*10^-4
dataset II
×10^4
Abundance
Time (hours)
WT, p=8.7*10^-12
CCA1-OX, p=0.034
B AT4G17090, BETA-AMYLASE 3
dataset I
×10^5
Abundance
Time (hours)
WT, p=0.0056
CCA1-OX, p=1.0
dataset II
×10^4
Abundance
Time (hours)
WT, p=4.6*10^-5
CCA1-OX, p=0.63
C AT2G05070, LHCB2.2
dataset I
×10^7
Abundance
Time (hours)
WT, p=0.013
CCA1-OX, p=1.0
dataset II
×10^6
Abundance
Time (hours)
WT, p=3.2*10^-4
CCA1-OX, p=0.076

bioRxiv preprint doi: https://doi.org/10.1101/760892; this version posted April 25, 2021. The copyright holder for this preprint (which was not certified by peer review) is the author/funder, who has granted bioRxiv a license to display the preprint in perpetuity. It is made available under aCC-BY-NC-ND 4.0 International license.

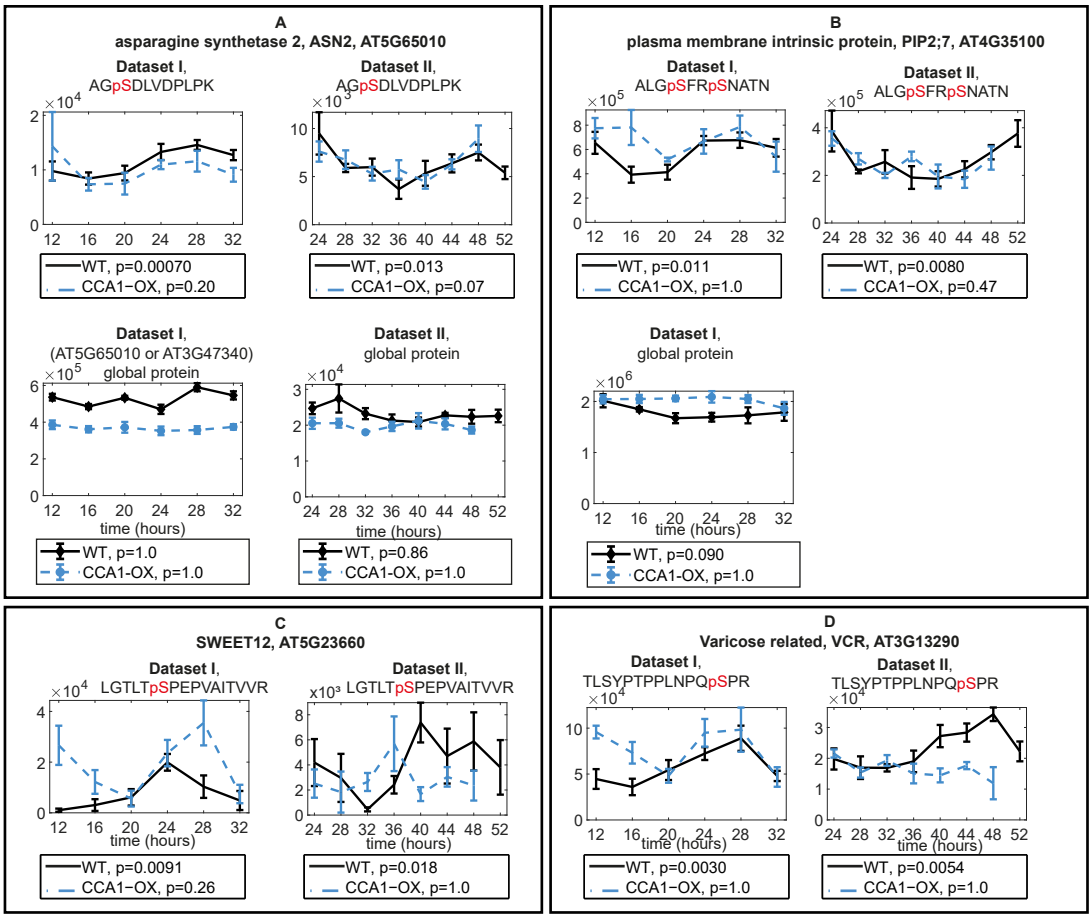

bioRxiv preprint doi: https://doi.org/10.1101/760892; this version posted April 25, 2021. The copyright holder for this preprint (which was not certified by peer review) is the author/funder, who has granted bioRxiv a license to display the preprint in perpetuity. It is made available under aCC-BY-NC-ND 4.0 International license.

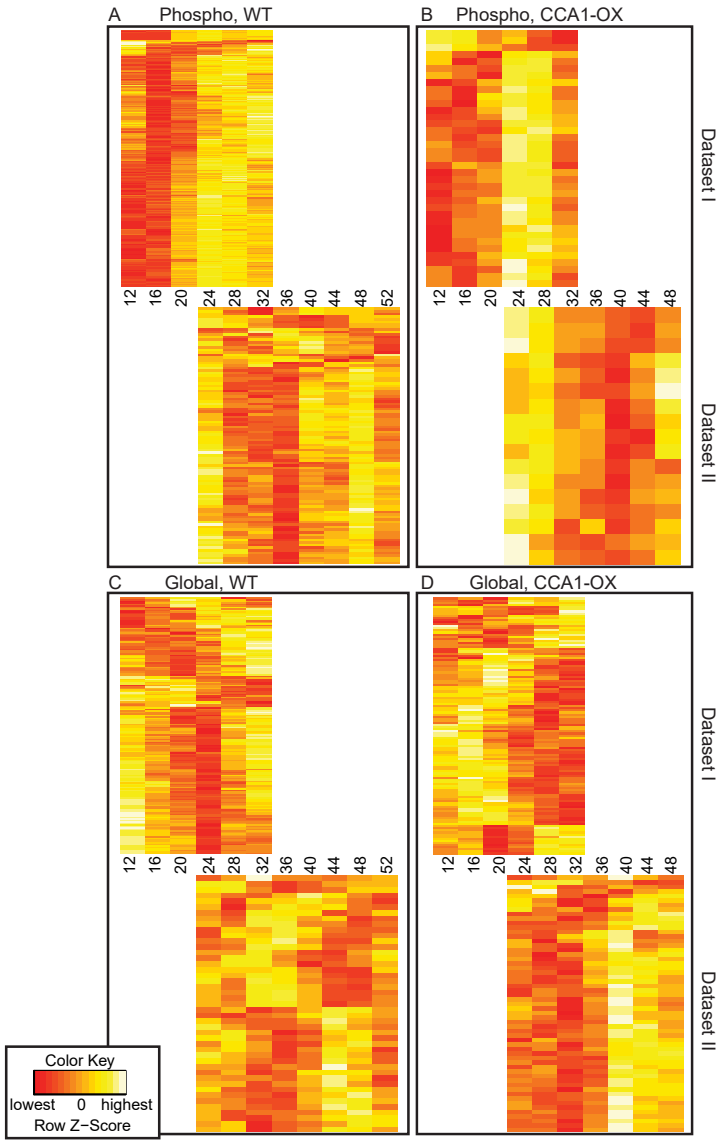

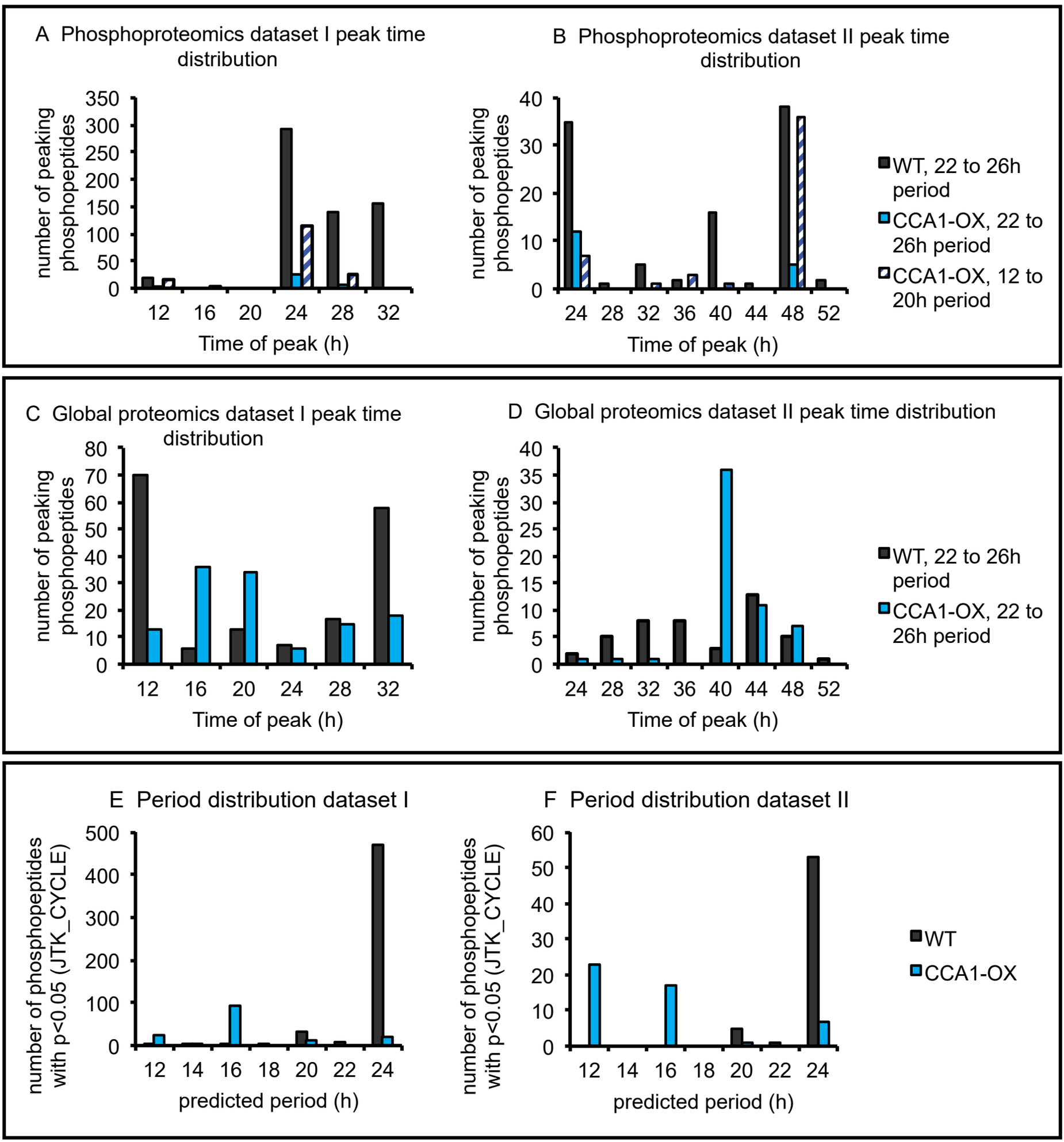
A Phosphoproteomics dataset I peak time distribution
number of peaking phosphopeptides
350
300
250
200
150
100
50
0
12 16 20 24 28 32
Time of peak (h)
B Phosphoproteomics dataset II peak time distribution
number of peaking phosphopeptides
40
30
20
10
0
24 28 32 36 40 44 48 52
Time of peak (h)
WT, 22 to 26h period
CCA1-OX, 22 to 26h period
CCA1-OX, 12 to 20h period
C Global proteomics dataset I peak time distribution
number of peaking phosphopeptides
80
70
60
50
40
30
20
10
0
12 16 20 24 28 32
Time of peak (h)
D Global proteomics dataset II peak time distribution
number of peaking phosphopeptides
40
35
30
25
20
15
10
5
0
24 28 32 36 40 44 48 52
Time of peak (h)
WT, 22 to 26h period
CCA1-OX, 22 to 26h period
E Period distribution dataset I
number of phosphopeptides with p<0.05 (JTK_CYCLE)
500
400
300
200
100
0
12 14 16 18 20 22 24
predicted period (h)
F Period distribution dataset II
number of phosphopeptides with p<0.05 (JTK_CYCLE)
60
50
40
30
20
10
0
12 14 16 18 20 22 24
predicted period (h)
WT
CCA1-OX

bioRxiv preprint doi: https://doi.org/10.1101/760892; this version posted April 25, 2021. The copyright holder for this preprint (which was not certified by peer review) is the author/funder, who has granted bioRxiv a license to display the preprint in perpetuity. It is made available under aCC-BY-NC-ND 4.0 International license.